sustainability

MDPI

Article

Optimisation of Building Green Performances Using Vertical Greening Systems: A Case Study in Changzhou, China

Yue Yang [1,2], Kai Hu [2], Yibiao Liu [1,2], Zhihuang Wang [2], Kaihong Dong [2], Peijuan Lv [2] and Xing Shi [3,4,*]

[1] Jiangsu Research Institute of Building Science Co., Ltd., Nanjing 210008, China
[2] Jiangsu Jianke Identification Consulting Co., Ltd., Nanjing 210008, China
[3] College of Architecture and Urban Planning, Tongji University, Shanghai 200092, China
[4] Key Laboratory of Ecology and Energy-Saving Study of Dense Habitat, Ministry of Education, Shanghai 200092, China
* Correspondence: 20101@tongji.edu.cn; Tel.: +86-021-65980048 (ext. 220)

Abstract: The benefits of greening systems on buildings have been frequently examined using experimental methods. However, few studies have adopted dynamic monitoring of real operational buildings to quantify the effects of greening systems on multiple building green performance indexes, such as thermal comfort, indoor air quality, and energy consumption. In this study, a type of multi-in-one indoor environmental quality monitoring device was adopted for vertical greening systems in a green-certified building in Changzhou, China, with real-time data collection through an Internet of Things platform. Measurements of the indoor thermal environment and air quality were recorded from four testing points during a 90 day period from spring to summer in 2021. For comparison, the testing points were divided into group A (office zone) and group B (exhibition zone). Our results demonstrated that, in the presence of a vertical greening system, the seasonal average indoor temperatures decreased by up to 0.7 °C. The green facade outperformed the ordinary exterior wall, optimising both indoor thermal comfort and thermal inertia. Furthermore, judicious indoor greening designs significantly reduced the indoor air-pollutant concentrations, such as particulate matter, carbon dioxide, and organic pollutants. The median values for particulate matter 10 and formaldehyde concentration decreased by 20.7% and 33.3%, respectively, thus improving the indoor air quality. Lastly, the annual electricity consumption of the building with vertical greening systems was about 25% lower than that of similar buildings, underlining the potential contribution of vertical greening systems to building energy conservation. Such findings collectively demonstrate that greening systems offer quantifiable benefits for building parameters such as thermal properties, indoor air quality, and energy conservation.

Keywords: vertical greening system (VGS); building green performance; real-time monitoring; thermal environment; indoor air quality; energy conservation

Citation: Yang, Y.; Hu, K.; Liu, Y.; Wang, Z.; Dong, K.; Lv, P.; Shi, X. Optimisation of Building Green Performances Using Vertical Greening Systems: A Case Study in Changzhou, China. *Sustainability* **2023**, *15*, 4494. https://doi.org/10.3390/su15054494

Academic Editor: Dušan Katunský

Received: 13 January 2023
Revised: 23 February 2023
Accepted: 24 February 2023
Published: 2 March 2023

1. Introduction

Augmenting the greenery of buildings has been demonstrated to critically mitigate the adverse effects of global warming and rapid urban densification [1], such as the urban heat island effect [2], diminished water availability [3], and deteriorating air pollution [4]. Infrastructural overcoats employing greening systems not only reduce the damage caused by concrete buildings to the ecological environment but also restore damaged ecological spaces [5]. However, as urban expansion and development continue unabated, the scale of urban greenery has become increasingly subject to space constraints. While traditional greening systems principally include on-site green squares and courtyards, a relatively novel strategy in recent decades is vertical greening systems (VGSs), which hold promising potential considering their convenience and spatial compactness [6].

VGSs comprise three categories: green walls (GWs), green facades (GFs), and living wall systems (LWSs). Apart from diversifying architectural landscapes, the benefits of VGSs

are threefold: they improve indoor thermal comfort, promote air purification and removal of pollutants, and enable energy savings for the cooling and heating of buildings [1].

1.1. Improving Indoor Thermal Comfort

Notably, VGSs provide passive indoor and outdoor cooling without occupying valuable urban land space, thus mitigating thermal environmental deterioration in contemporary urbanised settings. The cooling and heating performances of VGSs for buildings have been widely reported in previous studies [7] via different methods (empirical and simulated) [8]. In one study, VGSs were experimentally found to improve indoor thermal environments and lessen the use of air conditioning in summer [9]. In another study on the effects of different plants on cooling air internally and externally, VGSs were experimentally shown to reduce air temperatures by at least 1.0 °C in summer as compared to bare buildings [10]. Such empirical findings have been corroborated by simulation-based research: a virtual EnergyPlus model based on thermal-balance principles found that simulated VGSs lowered external surface temperatures of building walls in summer [11].

More specifically, some studies have increasingly focused on unconditioned buildings with greenery for summer periods. Investigations of a vegetation layer in a continental Mediterranean climate during summer found that the layer decreased the indoor dry bulb temperature by 4.0 °C on average [12]. Another study compared the thermal environments of chambers with and without an LWS, reporting that the indoor dry bulb temperature of the chamber with the LWS decreased by 1.1 °C during summer [13]. Additionally, evidence has demonstrated that indoor dry bulb temperatures in an unconditioned building could be diminished by 0.6 to 1.2 °C using VGSs [7].

The impacts of VGSs on indoor thermal environments vary critically with seasons [14]. However, to the best of our knowledge, few studies have hitherto investigated such impacts during transition seasons.

1.2. Promoting Air Purification and Removal of Pollutants

More than 80% of humans' time is spent indoors [1], and indoor air is at least twice as polluted as outdoor air, with consequent health risks from long-term exposure to indoor air pollution [1]. These findings have thus led to demands for improvements in indoor air quality (IAQ). Against this background, experimental results have demonstrated the utility of indoor greening in reducing indoor CO_2 concentrations, mould spores, and particulate matter [15]. Research on pollutant reduction using VGSs can be divided into three categories: theoretical, experimental, and model-based. Theoretical and experimental studies examine the physical factors that govern the capture of pollutants by plants, such as the built environment, plant morphology, and leaf area index. Findings from such studies can then be employed to validate any proposed modelling of plant-mediated pollutant reduction.

In this context, some theoretical and experimental findings from the literature have suggested that plants with trichome leaves are effective particulate-matter filters [16]. Furthermore, most particulate pollutants removed by plants have larger sizes [17]. A minority of particulate pollutants have small sizes [18]. Ysebaert et al. [19] simulated the mechanism underlying particulate-matter deposition and the influence of vegetation characteristics on this process, suggesting the potential of VGSs for the removal of particulate matters. Feng [20] established a VGS model for indoor air purification to quantify the total capture of NO_2, SO_2, O_3, and PM_{10}. The authors adopted the experimental results for an average green roof as their validation data [21]. An overview of the different modelling techniques has been put forward in [22]. In general terms, it is necessary to develop more models that quantify VGS-mediated air-pollution reductions in terms of both particulate-matter uptake and adsorption of gaseous pollutants from atmospheric air. However, it should be recognised that few experiments have been conducted on indoor pollutants, since it is unclear whether the scale of greening critically governs the air-cleaning potential per unit area [23].

1.3. Enabling Energy Savings in the Cooling and Heating of Buildings

VGSs not only improve thermal comfort but also reduce energy consumption arising from refrigeration [24–28]. In some studies, VGSs were modelled as a single thermal resistance added to a building envelope [29]; upon calculation of the thermal resistance from the thermal conductivity and the thickness of each component (including the plants), the VGSs were found to enable energy savings of 26.9% [30]. In another study, the VGS registered energy savings of 58.9% in buildings [8]. Further experimental evidence has also been reported for summers. A Hong Kong-based study on potential energy savings for cooling over the summer reported total savings of 134 kWh, which represented annual savings of 15.8% [31]. Notably, researchers in another study adopted their own experimental set-up to determine energy savings with VGSs, demonstrating substantial energy reductions in summer months [32].

A literature review [1] found that less attention has been paid to the impacts of VGSs on indoor environments than those on energy performances. It is crucial to recognise that indoor environments govern not only residents' health but also energy consumption [33]. Furthermore, such effects of VGSs have rarely been examined in the context of real buildings due to the lack of relevant data for such buildings and the complex interplay between these effects. Additionally, existing studies have largely focused on such environments during summer but not in transition seasons. However, weather fluctuations during transition seasons typically induce severe oscillations and alterations in indoor thermal environments, causing human discomfort, short-cycling of air-conditioning systems, and switching between heating and cooling demands. It is thus significant to investigate indoor thermal environments in transition seasons.

1.4. Research Gaps and the Aim of the Study

Most existing VGS-related studies were based on experiments or simulations and only focused on a number of indicators in a single field. To the best of our knowledge, few studies have examined all three of the abovementioned benefits of VGSs in actual buildings. Against this background, this study examined external and indoor VGSs in actual building operations with the aim of analysing whether VGSs would enable quantifiable improvements in the indoor thermal environments of buildings, indoor air quality, and energy conservation.

It is worth noting that this research was based on an actual operational building under the influences of complex factors, and the experimental measurements might not have been as rigorous as laboratory-based ones. However, quantitative case studies on the real-time monitoring and energy consumption of building operations are necessary to provide insights into the actual effects of VGSs on building green performances.

To this end, the following research questions were formulated:

(1) What are the differences in the indoor thermal environment and the air quality between a room with VGSs and a room without VGSs?
(2) Do VGSs contribute to energy conservation in actual building operations?

2. Materials and Methods

2.1. Project Information

The geographical site of interest in our study, Hengtang River Wetland Park in Changzhou City (Figure 1A), is located in the centre of the Yangtze River Delta (Figure 1B), one of the regions in China with the most widespread implementation of green buildings. Changzhou is located in a hot summer and cold winter climate zone. It is further characterised by a humid monsoon climate, four distinct seasons, simultaneous rain and heat, and sufficient sunlight. Statistical data from the Changzhou Meteorological Bureau showed that the average annual temperature in Changzhou from 1952 to 2021 was 16.1 °C. The Changzhou Ecological Environment Bulletin 2021 reported a total of 279 days with good air quality in the urban area of Changzhou in 2021, and the rate of good air quality was 76.4%. Within the Yangtze River Delta region, green building areas have grown by over

200 million square meters annually in recent years, exceeding 2 billion square meters at the end of 2021 [34].

(A)

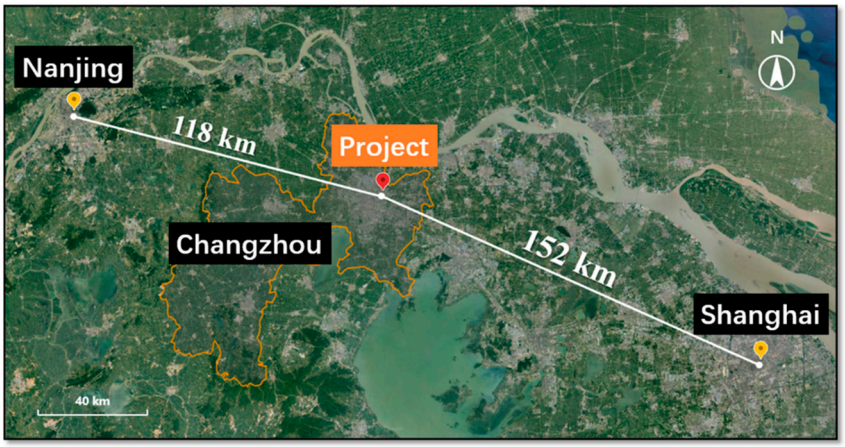

(B)

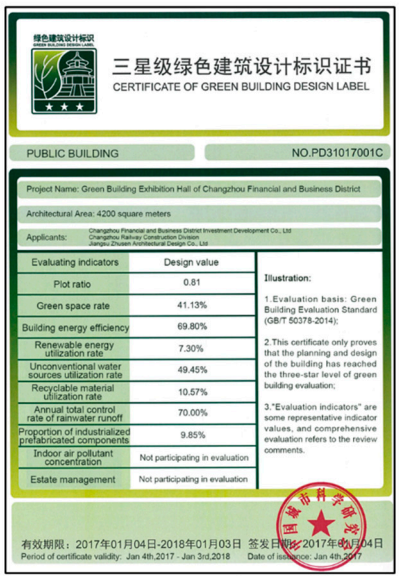
三星级绿色建筑设计标识证书
CERTIFICATE OF GREEN BUILDING DESIGN LABEL

PUBLIC BUILDING NO.PD31017001C

Project Name: Green Building Exhibition Hall of Changzhou Financial and Business District

Architectural Area: 4200 square meters

Applicants: Changzhou Financial and Business District Investment Development Co., Ltd; Changzhou Railway Construction Division; Jiangsu Zhusen Architectural Design Co., Ltd

Evaluating indicators	Design value
Plot ratio	0.81
Green space rate	41.13%
Building energy efficiency	69.80%
Renewable energy utilization rate	7.30%
Unconventional water sources utilization rate	49.45%
Recyclable material utilization rate	10.57%
Annual total control rate of rainwater runoff	70.00%
Proportion of industrialized prefabricated components	9.85%
Indoor air pollutant concentration	Not participating in evaluation
Estate management	Not participating in evaluation

Illustration:

1.Evaluation basis: Green Building Evaluation Standard (GB/T 50378-2014);

2.This certificate only proves that the planning and design of the building has reached the three-star level of green building evaluation;

3."Evaluation indicators" are some representative indicator values, and comprehensive evaluation refers to the review comments.

有效期限：2017年01月04日-2018年01月03日 签发日期：2017年01月04日

Period of certificate validity: Jan 4th,2017 - Jan 3rd,2018 Date of issuance: Jan 4th,2017

(C)


NO.PO31021020

三星级绿色建筑标识证书

CERTIFICATE OF GREEN BUILDING LABEL

Project Name: Green Building Exhibition Hall of Changzhou Financial and Business District

Architectural Area: 4200 square meters Building Type: Public Building

Applicants: Changzhou Financial and Business District Investment Development Co., Ltd; Jiangsu Research Institute of Building Science Co., Ltd; Jiangsu Zhusen Architectural Design Co., Ltd

Evaluating indicators	Design value	Measured value
Building energy efficiency	69.18%	69.18%
Renewable energy utilization rate	7.30% (Solar PV)	6.46% (Solar PV)
Unconventional water sources utilization rate	49.45%	9.70%
Green space rate	37.13%	37.13%
Recyclable material utilization rate	10.57%	10.50%
Indoor air pollutant concentration	Not participating in evaluation	Accord with GB/T 18883
Estate management	Not participating in evaluation	ISO14001,ISO9001, GB/T 23331 certified

Illustration:

1.Evaluation basis: Green Building Evaluation Standard (GB/T 50378-2014);

2."Evaluation indicators" are some representative indicator values, and comprehensive evaluation refers to the review comments.

发证日期：2021年05月31日

Date of issuance: May 31st , 2021

(D)

Figure 1. Green certification and geographical information. (**A**) Project aerial map, (**B**) project location analysis, (**C**) three-star green-building design label, (**D**) three-star green-building operating label.

The roof and exterior-wall thermal insulation materials used in the project are made of expanded polystyrene (EPS) boards. The heat transfer coefficients for the roof and exterior wall are 0.39 W/(m^2·K) and 0.63 W/(m^2·K), respectively. The outer windows employ three layers of glass and heat-insulating metal profiles, with the heat transfer coefficient reaching 1.8 W/(m^2·K) in the east and 2.1 W/(m^2·K) in the other directions. On this basis, the thermal performance of the enclosure conforms to the relevant provisions from energy-saving design standards. The air conditioning system used in the project employs variable refrigerant volume (VRV) technology, and the integrated part load value (IPLV) is above 7.0. In order to save energy, LED light sources are used in the building, while centralized control, zoning control, and induction control measures are adopted for public area lighting.

The building of interest in this study has two floors with an area of 4334.71 m^2, including 3952.86 m^2 overground and 381.85 m^2 underground. First completed and put into use in 2019, it has primarily been used for offices (2204.07 m^2) and exhibition halls (1748.79 m^2). A Chinese three-star green-building design label was awarded to this building in 2017 (Figure 1C), followed by a three-star green-building operating label in 2021 (Figure 1D) (three stars is the highest level in the Chinese assessment standard for green buildings).

In our experimental set-up, VGSs were mounted on both the west exterior wall and the interior atrium (Figure 2): the external VGS area measured 223 m^2, while the indoor one measured 132 m^2. In this system, a paving-type flexible support was attached onto the base wall alongside planting bags fixed to the wall surfaces (Figure 3). Anti-ultraviolet planting-bag technology was adopted for the outdoor green planting wall that could reach a service life exceeding 10 years under plant coverage. At the top of the green wall, a root-irrigation pipe network was installed from which water would be released to infiltrate the system layer by layer for plant growth, while a micro-control system was configured for automatic irrigation.

Crucially, the VGS-mediated improvement of the building green performances was supplemented with other purposes, such as enrichment of the spatial landscape, energy conservation, environmental protection, and regulation of building microclimates. In our investigations, long-term monitoring was designed by setting up multiple observation points and comparing groups for data collection so as to quantitatively appraise the effects of VGSs on building green performances.

(A)

(B)

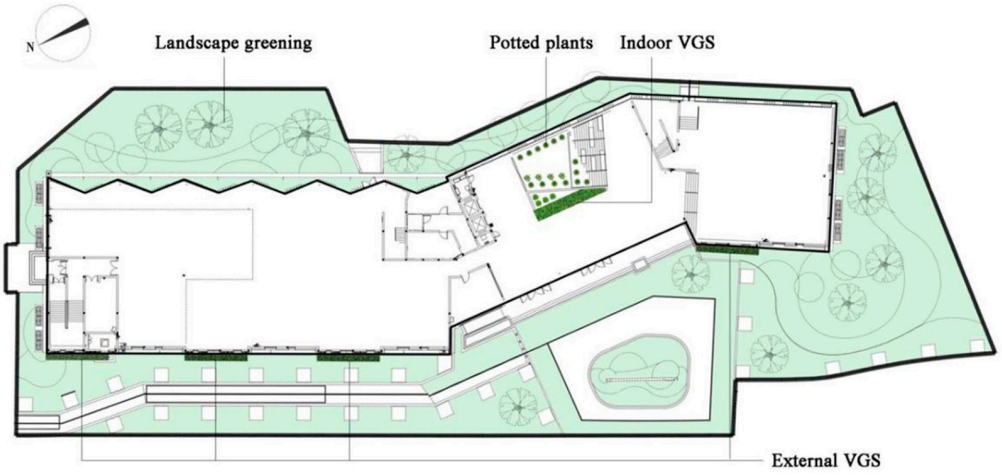

(C)

Figure 2. Building design diagrams showing greening systems. (**A**) Building design scheme (view of the west facade), (**B**) west facade design (indicating vertical greening areas), (**C**) general layout (indicating landscape greening, external VGS, indoor VGS, and indoor potted plants).

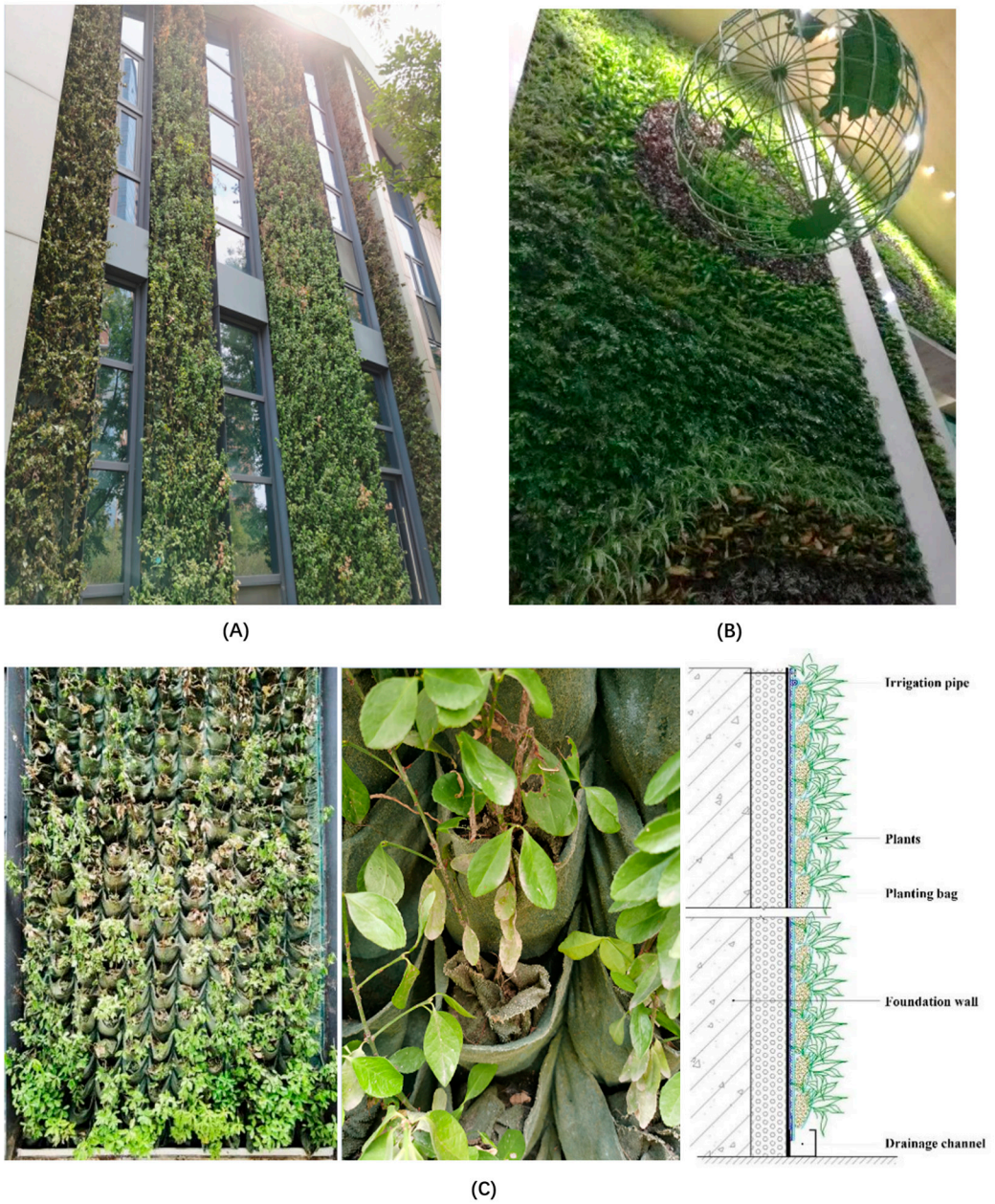

Figure 3. Vertical greening systems in this project. (**A**) Photo of the external VGS on the west facade, (**B**) photo of the indoor VGS in the interior atrium, (**C**) photos and structural drawing of planting bags in the VGS.

2.2. Experimental Description

The experiment spanned a 90 day period from 24 April to 22 July 2021 and took place in Changzhou in the hot summer and cold winter climate zone of China. Measurements of the indoor thermal environment and air quality were taken at four testing points across the building interior space, which was divided into the office zone and exhibition zone (Figure 4). Throughout the experiment, the office zone was operating from 7:00 a.m. to 7:00 p.m. on weekdays, whereas the exhibition zone was closed. Air conditioning systems in the two zones operated independently, and the exhibition zone was kept in the free-running mode without air conditioning.

Figure 4. *Cont.*

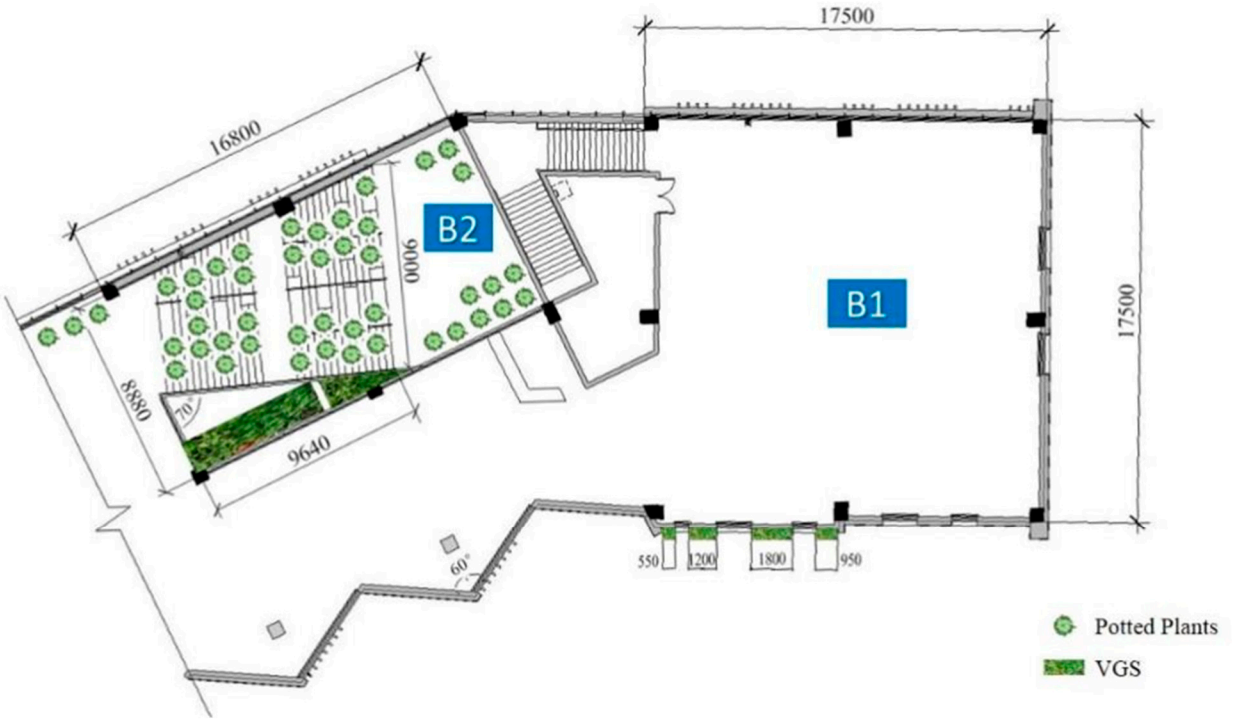

(D)

(E)

Figure 4. Description of comparison groups. (**A**) Floor plans indicating the functional areas and locations of the testing points, (**B**) floor plan of group A, (**C**) photo of group A, (**D**) floor plan of group B, (**E**) photos of group B.

The four testing points were divided into two comparison groups to examine the different aspects of the VGSs. In the office zone, rooms 210 (A1) and 212 (A2) were set as a comparison group (group A) to analyse the effects of the external VGS. In the exhibition zone, the exhibition hall (B1) and atrium (B2) were set as another comparison group (group B) to evaluate the effects of the VGS on the IAQ in addition to thermal properties (Table 1).

Table 1. Comparison group information and evaluation aspects.

Group ID	Point ID	Point Location	Functional Area	External VGS	Indoor VGS	Evaluation Aspect
Group A	A1	Meeting room 210, 2nd floor	Office zone	×	×	Thermal properties
	A2	Meeting room 212, 2nd floor		○	×	
Group B	B1	Exhibition hall, 1st floor	Exhibition zone	○	×	IAQ and thermal properties
	B2	Atrium		×	○	

Note: ○ indicates that the room had a VGS. × indicates that the room lacked a VGS.

In the office zone, rooms A1 and A2 were both meeting rooms with identical areas (75 m^2). A questionnaire-based survey [35] was conducted to investigate the occupancy of the rooms by office users. It was found that these meeting rooms were not frequently in use (they were occupied for about only 10% of the time during the experiment). Since doors and windows were closed for most of the time during the testing periods, their negligible influences were not considered in this research. For both rooms, air conditioning was used during summer but not during the transitional season. They both faced the west, and their exterior walls were located on their western sides. In other words, the orientations, areas, functions, and operation modes of A1 and A2 were similar; the crucial difference was that a VGS was installed on the external wall face of A2 but not A1. The area of this external VGS for A2 was 31.1 m^2, accounting for 61.1% of its total exterior wall area. Accordingly, the experimental set-up for group A focused on the effects of the external VGS on the indoor thermal environment.

In the exhibition zone, the exhibition hall (B1) and atrium (B2) were analysed. No exhibitions were held throughout the experiment, and the air conditioning was rarely in use. B1 occupied an area of 364.8 m^2, and its three exterior walls were, respectively, east-, south-, and west-facing. The west exterior wall of B1 was covered by a VGS with an area of 31.1 m^2, accounting for 30.5% of its total exterior wall area. For B1, there was no indoor greenery. In contrast, B2 occupied an area of 146.4 m^2 and faced eastwards, with its highest floor reaching 11.9 m (B2 was an elevated space). For B2, an indoor VGS (132.6 m^2) was mounted on the inner wall of the west side of its open stairs, and potted plants were installed in groups on the steps of the stairs; there was no exterior greenery. In other words, the scales, functions, and operation modes of B1 and B2 were similar. The crucial difference related to the presence or absence of an indoor VGS. Accordingly, the experimental set-up for group B focused on the effects of the indoor VGS on the IAQ. Another less crucial difference related to the presence or absence of an external VGS. However, given the low coverage ratio of the external VGS of B1, the data on the indoor thermal environment of group B did not represent our principal focus, although they were analysed.

2.3. Data Processing

2.3.1. Measuring Indicators

Indoor environmental indicators (IEQs) encompass parameters such as thermal aspects, IAQ, lighting, and acoustics, for which evaluation methods may include objective physical measurements and subjective occupant surveys. For the Changzhou green building exhibition gall, seven IEQs were measured using Internet of Things (IoT) monitoring: air temperature, relative humidity, $PM_{2.5}$, PM_{10}, TVOC, CH_2O, and CO_2. The range, accuracy, and other performance specifications of the sensors are detailed in Table 2.

Table 2. List of monitoring indicators with their performance specifications and application areas.

Parameter	Measurement Range	Resolution	Accuracy	Indoor Monitor	Outdoor Monitor
Air temperature (TEMP)	−40 °C~+120 °C	0.1 °C	±0.5 °C (25 °C)	○	○
Relative humidity (RH)	0% RH–100% RH	0.1% RH	±3% RH (60% RH, 25 °C)	○	○
Particulate matter 2.5 ($PM_{2.5}$)	0–1000 μg/m^3	1 μg/m^3	±10%	○	○
Particulate matter 10 (PM_{10})	0–1000 μg/m^3	1 μg/m^3	±10%	○	○
Total volatile organic compounds (TVOC)	0–60,000 μg/m^3	1 μg/m^3	±8% FS ± 125 μg/m^3	○	×
Formaldehyde (CH_2O)	0–1.50 mg/m^3	0.01 mg/m^3	±5% FS	○	×
Carbon dioxide (CO_2)	0–5000 ppm	1 ppm	±40 ppm ± 3% FS	○	×

Note: ○ indicates that the parameter was monitored. × indicates that the parameter was not monitored. 1 ppm = 0.001‰. FS, full scale.

A type of multi-in-one IEQ monitoring device (Figure 5A,C) was adopted in which sensors for the above seven IEQs were integrated into one consolidated box. An outdoor weather station (Figure 5B) was also used to monitor the atmospheric environmental indexes outdoors. The monitoring equipment for the indoor and outdoor environments is detailed in Table 2.

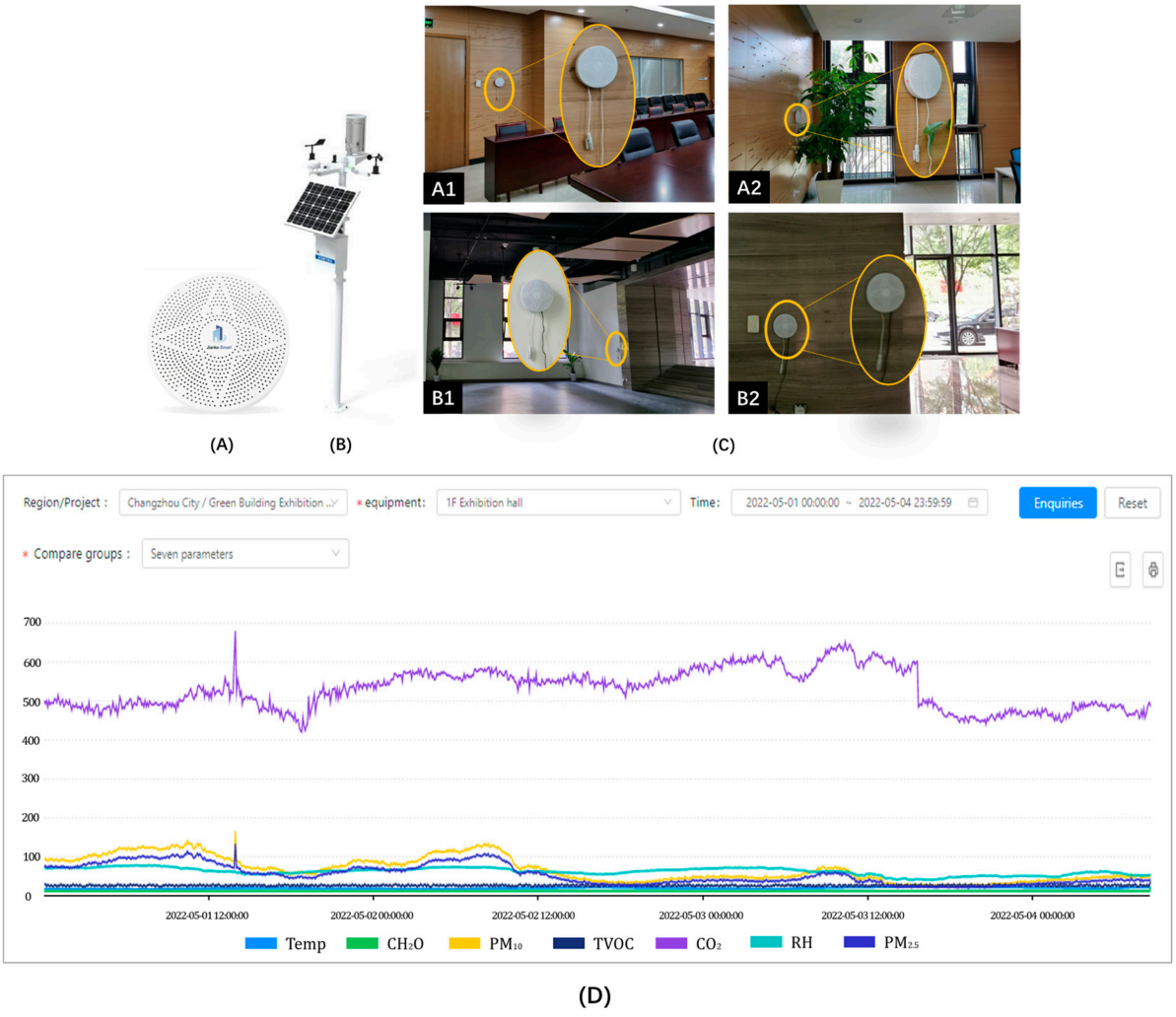

Figure 5. IoT-based environmental monitoring devices and platform. (**A**) Indoor air quality monitoring device, (**B**) outdoor weather station, (**C**) on-site devices, (**D**) data management platform.

2.3.2. IoT-Based Environmental Monitoring Platform

An IoT-based environmental monitoring platform was established that comprised sensor-monitoring terminals, a data-transmission system, and a back-end management system. Multi-point high-precision sensors were used to collect real-time environmental data, and IoT technologies were combined to achieve dynamic storage of data locally and in the cloud synchronously. The monitoring terminals used in this case integrated multiple sensors, including data for the IAQ and from the outdoor multi-functional weather station. Through the MQTT protocol, such terminals dispatched monitoring data at 5 min intervals to the back-end management system, which then managed the project equipment and queries and exported and analysed the data (Figure 5D).

2.4. Data Analysis

2.4.1. Statistical Analysis

The average values and trends for air temperature, relative humidity, and air quality were evaluated using curves to explain their behaviours under the influence of VGSs in groups A (A1 and A2) and B (B1 and B2). Moreover, the distributions of the IAQ indexes in group B were evaluated through box diagrams.

2.4.2. Thermal Comfort

Indoor thermal comfort was evaluated with an established method from ISO 7730 [36]. In this context, the PMV is an index that predicts the mean value of the votes on thermal sensation (self-reported perceptions) of a group of people. It uses a scale from −3 to +3 for thermal sensations: cold (−3), cool (−2), slightly cool (−1), neutral (0), slightly warm (1), warm (2), and hot (3). The PMV is calculated according to the thermal balance of the human body, which can be derived by estimating the rate of human metabolism and insulation due to clothing. Several environmental parameters are also required: air temperatures, radiant temperatures, air speeds, and humidity. In contrast, the PPD is an index that quantitatively predicts the percentage of thermally dissatisfied people as determined from the PMV.

The PMV can be calculated based on Equations (1)–(4):

$$\begin{aligned} PMV = [0.303\times \quad & \exp(-0.036M) + 0.028] \\ & \times\{(M-W) - 3.05\times10^{-3}[5733 - 6.99(M-W) - p_a] \\ & -0.42\times[(M-W) - 58.15] - 1.7\times10^{-5}M(5867 - p_a) \\ & -0.0014M(34 - t_a) - 3.96\times10^{-8}f_{cl}\left[(t_{cl}+273)^4 - (\bar{t}_r+273)^4\right] \\ & -f_{cl}h_c(t_{cl}-t_a)\} \end{aligned} \quad (1)$$

$$\begin{aligned} t_{cl} = 35.7 - 0.028(M-W) \\ -I_{cl}\left\{3.96\times10^{-8}f_{cl}\left[(t_{cl}+273)^4 - (\bar{t}_r+273)^4\right] + f_{cl}h_c(t_{cl}-t_a)\right\} \end{aligned} \quad (2)$$

$$h_c = \begin{cases} 2.38|t_{cl}-t_a|^{0.25} & \text{for} \quad 2.38|t_{cl}-t_a|^{0.25} > 12.1\sqrt{v_{ar}} \\ 12.1\sqrt{v_{ar}} & \text{for} \quad 2.38|t_{cl}-t_a|^{0.25} < 12.1\sqrt{v_{ar}} \end{cases} \quad (3)$$

$$f_{cl} = \begin{cases} 1.00 + 1.290I_{cl} & \text{for} \quad I_{cl} \le 0.078\ m^2\cdot K/W \\ 1.05 + 0.645I_{cl} & \text{for} \quad I_{cl} > 0.078\ m^2\cdot K/W \end{cases} \quad (4)$$

where M is the metabolic rate in watts per square meter (W/m^2); W is the effective mechanical power in watts per square meter (W/m^2); I_{cl} is the clothing insulation in square meters kelvin per watt ($m^2\cdot K/W$); f_{cl} is the clothing surface area factor; t_a is the air temperature in degrees Celsius (°C); $\bar{t}_r$ is the mean radiant temperature in degrees Celsius (°C); v_{ar} is the relative air velocity in meters per second (m/s); p_a is the water vapour partial pressure in pascals (Pa); h_c is the convective heat transfer coefficient in watts per square meter kelvin ($W/(m^2\cdot K)$); and t_{cl} is the clothing surface temperature in degrees Celsius (°C).

Based on the PMV value determined, the PPD was calculated using Equation (5):

$$PPD = 100 - 95\exp\left(-0.03353 \cdot PMV^4 - 0.2179 \cdot PMV^2\right) \quad (5)$$

2.4.3. Thermal Inertia

To further examine the effects of the VGSs on building thermal performances, the thermal inertia index of the reference group was analysed [37]. Detection of a delay in the comprehensive thermal inertia study of a given building indicates the response of the indoor air temperature under the joint influences of various factors. It is manifested as the delay between the peak and valley times for the indoor and outdoor air temperatures. This parameter reflects the hysteresis of air temperature waves: a larger value implies a greater delay in the air temperature waves and, hence, greater comprehensive thermal inertia for the building.

$$\varphi_{max} = \varphi_{max,in} - \varphi_{max,out} \quad (6)$$

$$\varphi_{min} = \varphi_{min,in} - \varphi_{min,out} \quad (7)$$

where φ_{max} is the maximum delay time, H; φ_{min} is the minimum delay time, H; $\varphi_{max,in}$ is the time with the maximum indoor air temperature, H; $\varphi_{max,out}$ is the time with the maximum outdoor air temperature, H; $\varphi_{min,in}$ is the time with the minimum indoor air temperature, H; and $\varphi_{min,out}$ is the time with the minimum outdoor air temperature, H.

When studying the comprehensive thermal inertia of buildings, the ratio of the difference between the maximum and minimum indoor air temperatures to the difference between the maximum and minimum outdoor air temperatures represents the coefficient of air temperature attenuation. A larger value for this parameter signifies smaller wave attenuation for indoor air temperatures and, hence, lower comprehensive thermal inertia for the building.

$$f = \frac{T_{max,in} - T_{min,in}}{T_{max,out} - T_{min,out}} \quad (8)$$

where $T_{max,in}$ is the maximum indoor air temperature, °C; $T_{min,in}$ is the minimum indoor air temperature, °C; $T_{max,out}$ is the maximum outdoor air temperature, °C; and $T_{min,out}$ is the minimum outdoor air temperature, °C.

3. Results

3.1. Thermal Environment

The effects of external and indoor greening on the thermal properties of the building were comparatively analysed. In group A, the external VGS was mounted in A2 but not A1; in group B, the indoor VGS and potted plants were mounted in atrium B2 but not the exhibition hall (B1). The paired rooms in both groups had similar space-usage modes, including personnel density, ventilation times, and fresh air system operation times. Two indicators (air temperature (Temp) and relative humidity (RH)) were measured using IoT-based outdoor and indoor monitoring from 24th April to 22nd July, spanning both spring and summer over a period lasting 90 days (2160 h). Raw data were pre-processed for this study, and the resultant data were then averaged by hour.

3.1.1. Outdoor Weather

During our case study, the average outdoor Temp was 25.3 °C (maximum: 37.0 °C; minimum: 14.2 °C), whereas the average RH was 64.6% (maximum: 100%; minimum: 23.3%) (Figure 6A,B). It is important to note that Changzhou belongs to the northern subtropical marine climate region, which has a mild climate, abundant rainfall, and distinct seasonality. Late spring and early summer in the region are known as the plum rain seasons and characterised by pronounced RH, while midsummer is hot and rainy. According to the standard from China's Climate Season Classification [38], outdoor air temperatures in the transition seasons range from 10.0 to 22.0 °C. The arrival of summer is typically marked by

five consecutive days during which the average outdoor air temperatures exceed 22.0 °C. In this context, the meteorological switch date (S-DAY) from spring to summer in 2021 was 26 May (Figure 6C), which was close to 22 May; i.e., the historical average date for Changzhou entering summer.

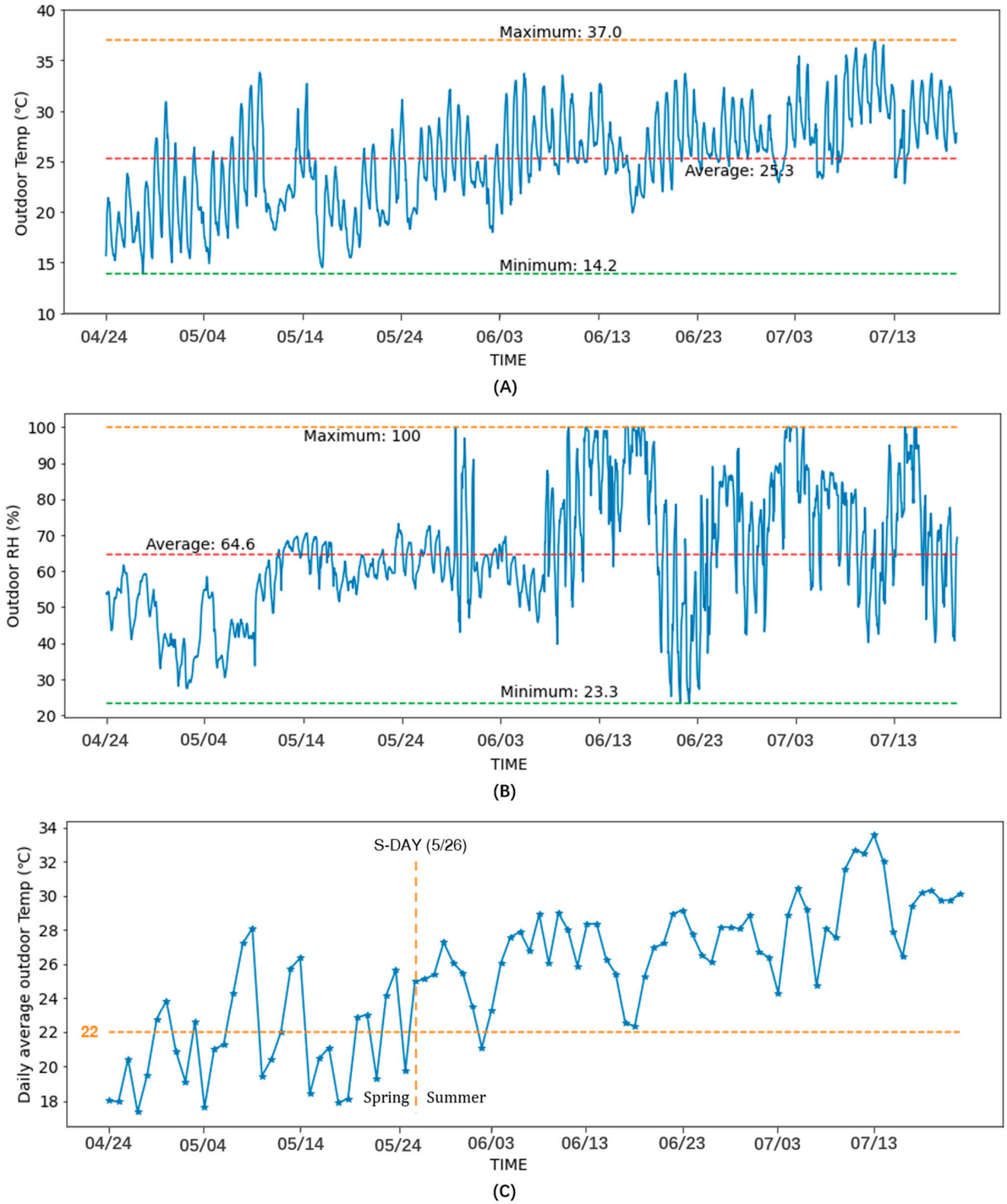

Figure 6. The curves for outdoor weather. (**A**) The curve for outdoor Temp, (**B**) the curve for outdoor RH, (**C**) the curve for daily averaged outdoor Temp.

3.1.2. Indoor Air Temperature

The indoor and outdoor air temperatures of groups A and B during the experiment are shown in Figure 7. The average values for A1 (without a VGS) and A2 (with a VGS) in

the transition season were, respectively, 22.8 °C and 22.1 °C, while those in summer were 26.9 °C and 27.1 °C (Figure 7A). As a result of the heat insulation capacity of the VGS, the average air temperature of A2 in the transition season was 0.7 °C lower than A1 and 2.5 °C higher than outdoors. Conversely, the average air temperature of A2 in summer was 0.2 °C higher than that of A1. The reason was that indoor air conditioning was in operation in summer, and the indoor air temperatures were thus unaffected by the building envelope. Accordingly, the indoor thermal environment of group A in summer will not be further analysed in this paper.

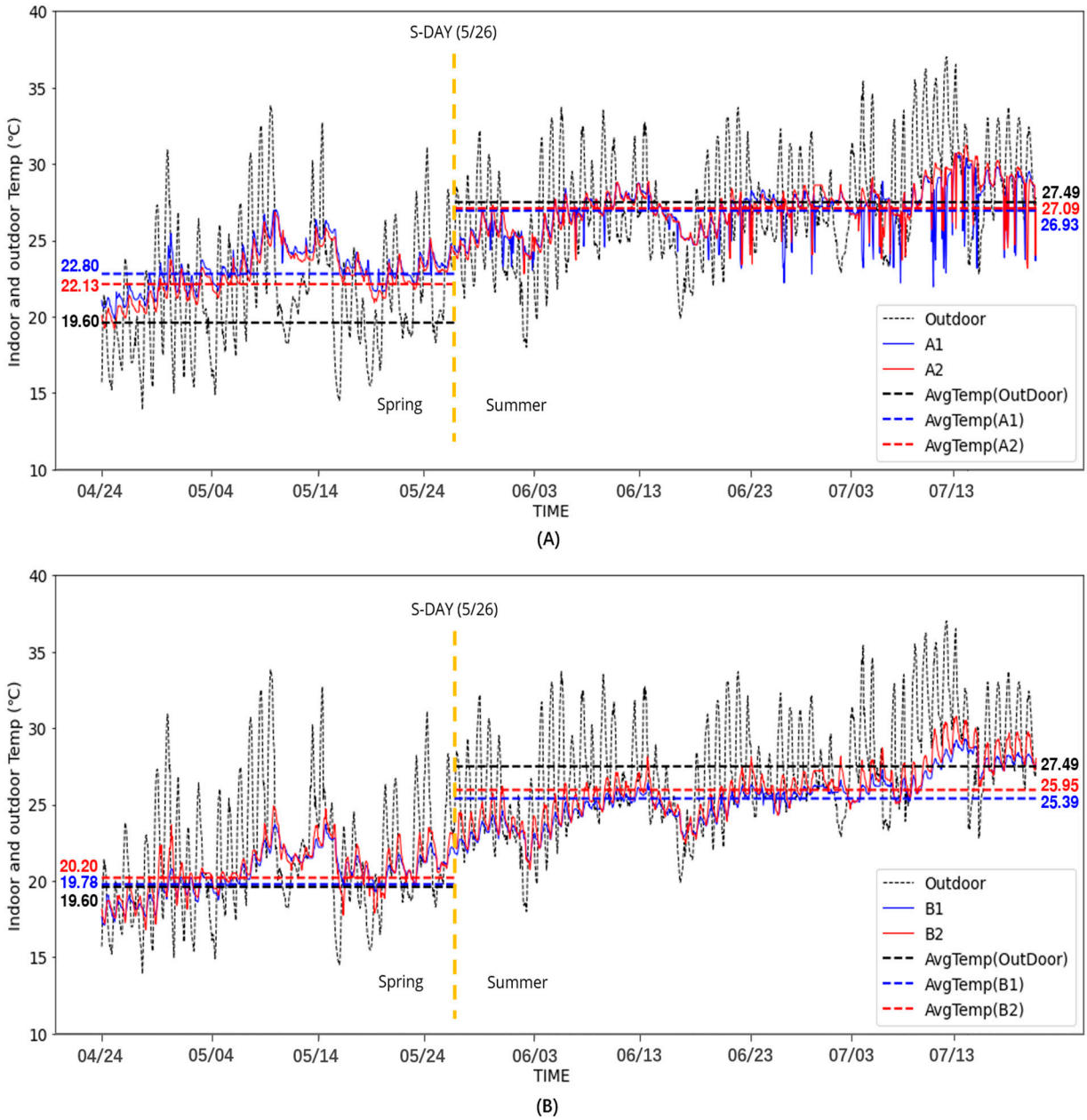

Figure 7. The comparison of indoor and outdoor air temperatures. (**A**) Group A, (**B**) group B.

The average values for B1 (with an external VGS) and B2 (with an indoor VGS) in the transition season were, respectively, 19.8 °C and 20.2 °C, and those in summer were 25.4 °C and 26.0 °C (Figure 7B). As a result of the heat insulation capacity of the VGS, the average air temperature of B1 in the transition season was 0.4 °C lower than that of B2 and that in

summer was 0.6 °C lower. These comparative findings demonstrate the indoor cooling effect exerted by the VGS.

Further analysis revealed that the oscillations in the indoor air temperatures in A1 and A2 in the transition season were less substantial than those in the outdoor air temperatures. For the two rooms, the oscillation amplitude in A2 was smaller than that in A1. Throughout the test period, the oscillations in indoor air temperatures in B1 and B2 were much less substantial than those in outdoor air temperatures. The oscillation amplitudes in B1 and B2 were similar. This suggested that the external VGS effectively reduced the oscillations in indoor air temperatures and improved the indoor thermal environment. However, there was no evidence that the indoor VGS outperformed the external VGS in reducing indoor air temperatures and mitigating indoor oscillations.

Since the site of interest was a three-star green building, the overall thermal performance of the building envelope was optimal, as inferred from the following heat transfer coefficients: roof—0.4 W/(m^2·K); external wall—0.6 W/(m^2·K); and external window—1.8 W/(m^2·K). Moreover, the site has adopted judicious adjustable sunshade measures. On this basis, the oscillations in the air temperatures at the measuring points with the external VGS were smaller than those without it. This highlighted that, given an enclosed structure with the same thermal performance, additional external VGSs could further optimise the indoor thermal environment. As exemplified by group A, given building envelopes with the same performances, the installation of a VGS could further diminish the ranges of the oscillations in the indoor air temperatures by 8.44%.

3.1.3. Indoor Relative Humidity

The indoor relative humidity (RH) of the rooms in groups A and B during the experiment (Figure 8) was critically governed by the climate of Changzhou, which is characterised by dry springs, humid plum rain seasons, and hot and rainy summers. Outdoor RH was found to fluctuate dramatically. During the transition season, the outdoor RH in spring, averaging 54.0%, was lower than the indoor average RH by about 7.8%. Conversely, during summer, the outdoor RH, averaging 71.1%, was higher than the indoor RH by about 3.5%.

Table 3 outlines the indoor and outdoor average RH levels in spring and summer for groups A and B, as well as the difference between the average RH levels in spring and summer (ΔRH). The results appeared to parallel the trend for air temperatures (see above), in that the ranges of the oscillations in the indoor RH were generally smaller than those for the outdoor RH. The outdoor ΔRH value reached 16.9%, whereas the four indoor ΔRH values were all below 9.0%. The ΔRH for A2 (with an external VGS) was 2.5% lower than that for A1, while the ΔRH for B2 (with an indoor VGS) was the lowest among the four indoor points. It was noteworthy that the range of oscillations in the RH for B2 (non-air conditioned) in summer was even smaller than that for group A (air conditioned). Such findings suggested that the indoor and external VGSs could stabilise the indoor RH, with indoor greening exerting a more pronounced effect.

Table 3. The average seasonal RH and the difference in RH between seasons.

Point ID	Spring Average RH (%)	Summer Average RH (%)	ΔRH (%)
A1	60.1	69.0	8.9
A2	63.1	69.5	6.4
B1	62.0	67.0	5.0
B2	61.8	65.1	4.3
Outdoor	54.0	71.1	16.9

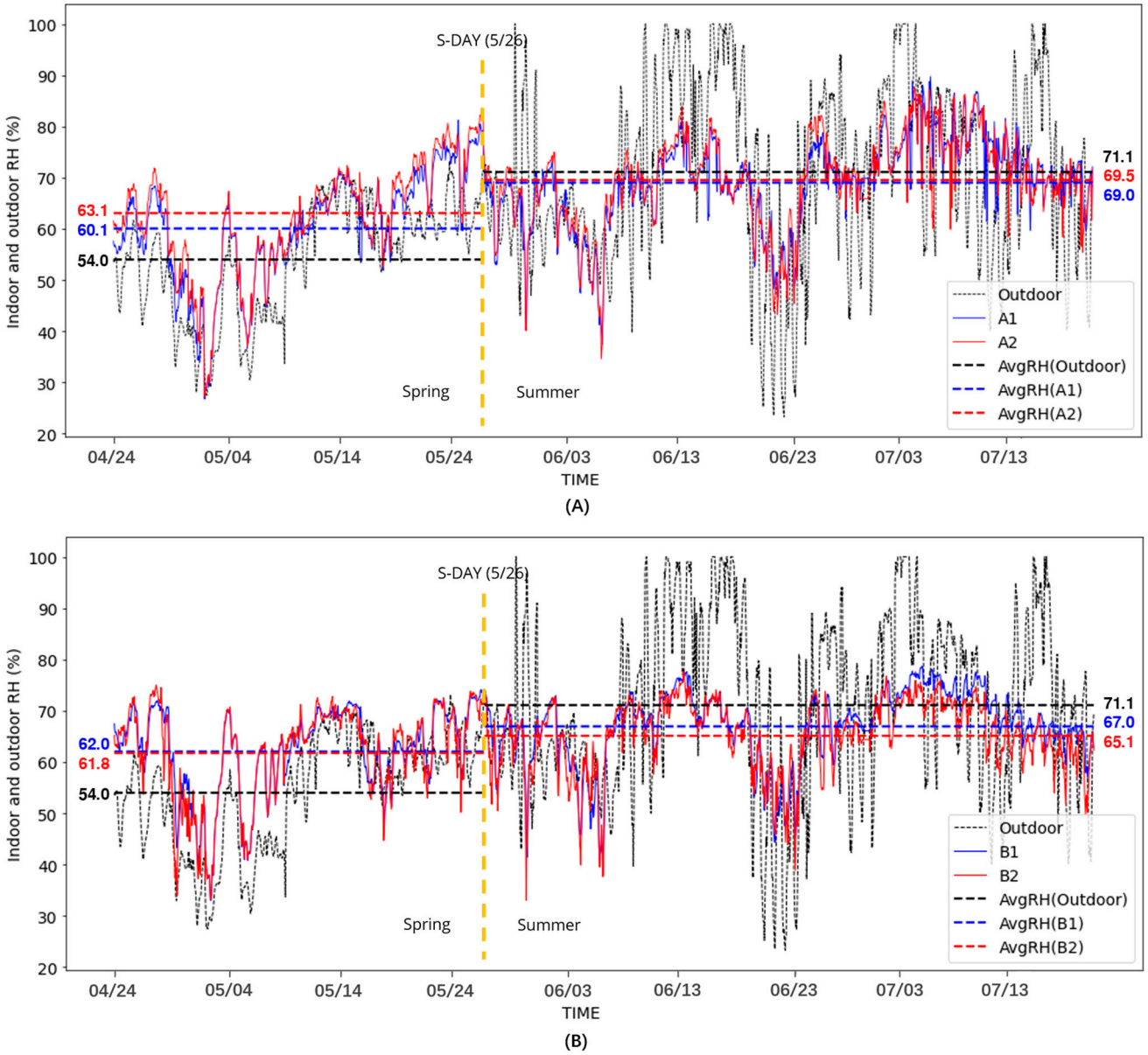

Figure 8. Comparison of indoor and outdoor RH. (**A**) Group A, (**B**) group B.

3.2. Indoor Air Quality

The effects of indoor greening on indoor air quality (IAQ) were comparatively analysed. In group B, the indoor VGS and potted plants were installed in the atrium (B2), whereas the exhibition hall (B1) had no indoor greenery. Both rooms in group B had similar space usage modes, including personnel density, ventilation times, and fresh air system operation times. Five IAQ indicators ($PM_{2.5}$, PM_{10}, CO_2, TVOC, and CH_2O) were measured through IoT-based monitoring from 24 April to 22 July (Figure 9). For concentrations of PM, both indoor and outdoor monitoring data were obtained; for concentrations of CO_2 and organic pollutants, only indoor data were obtained.

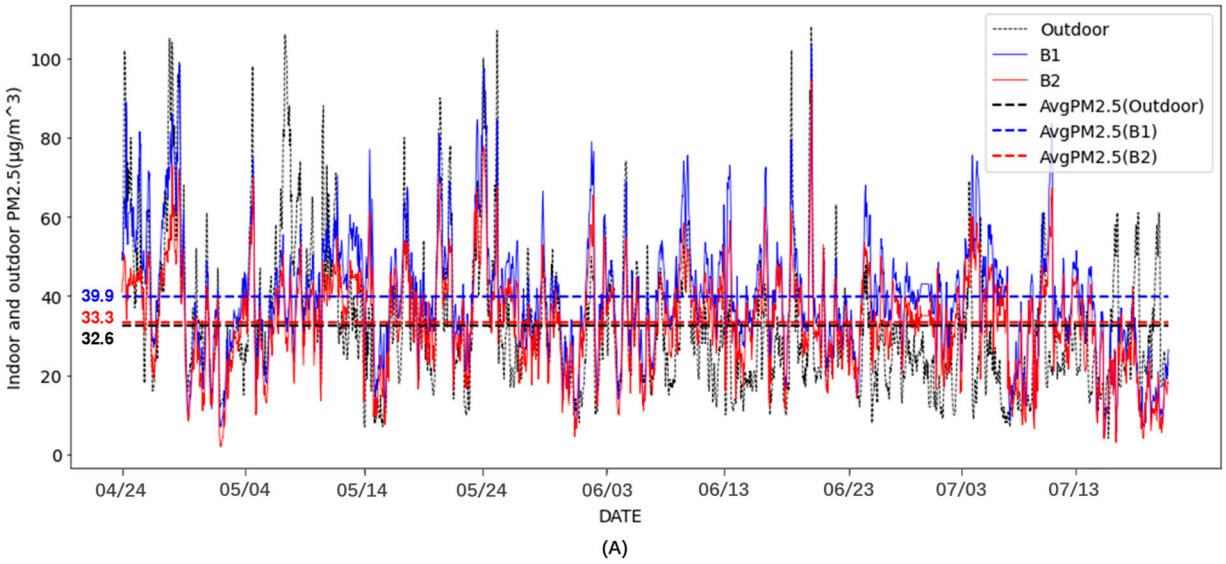

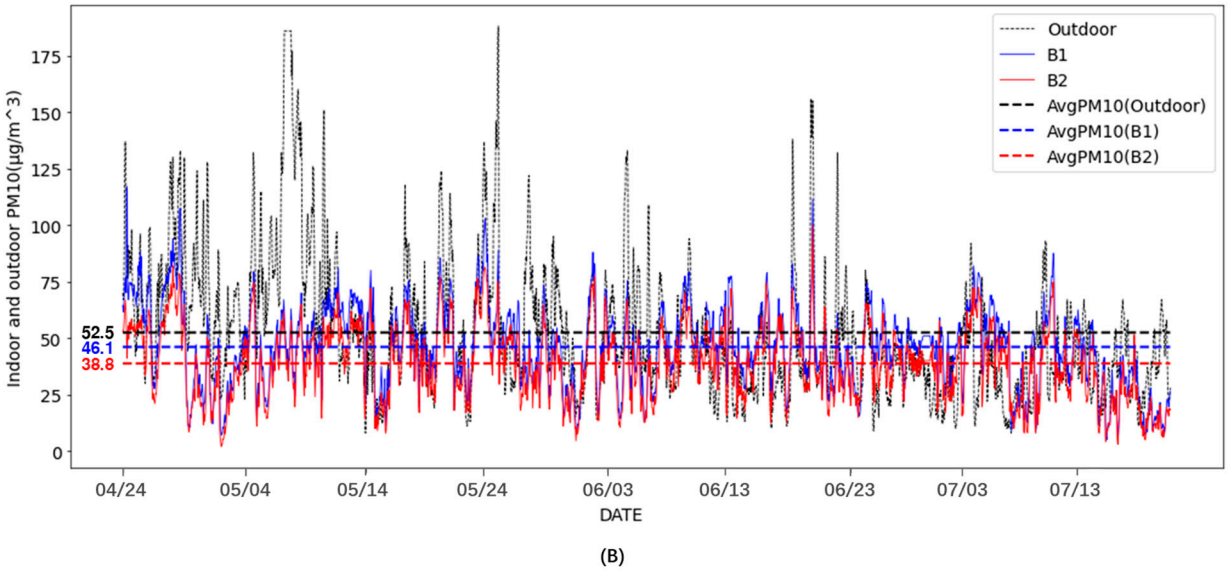

Figure 9. *Cont.*

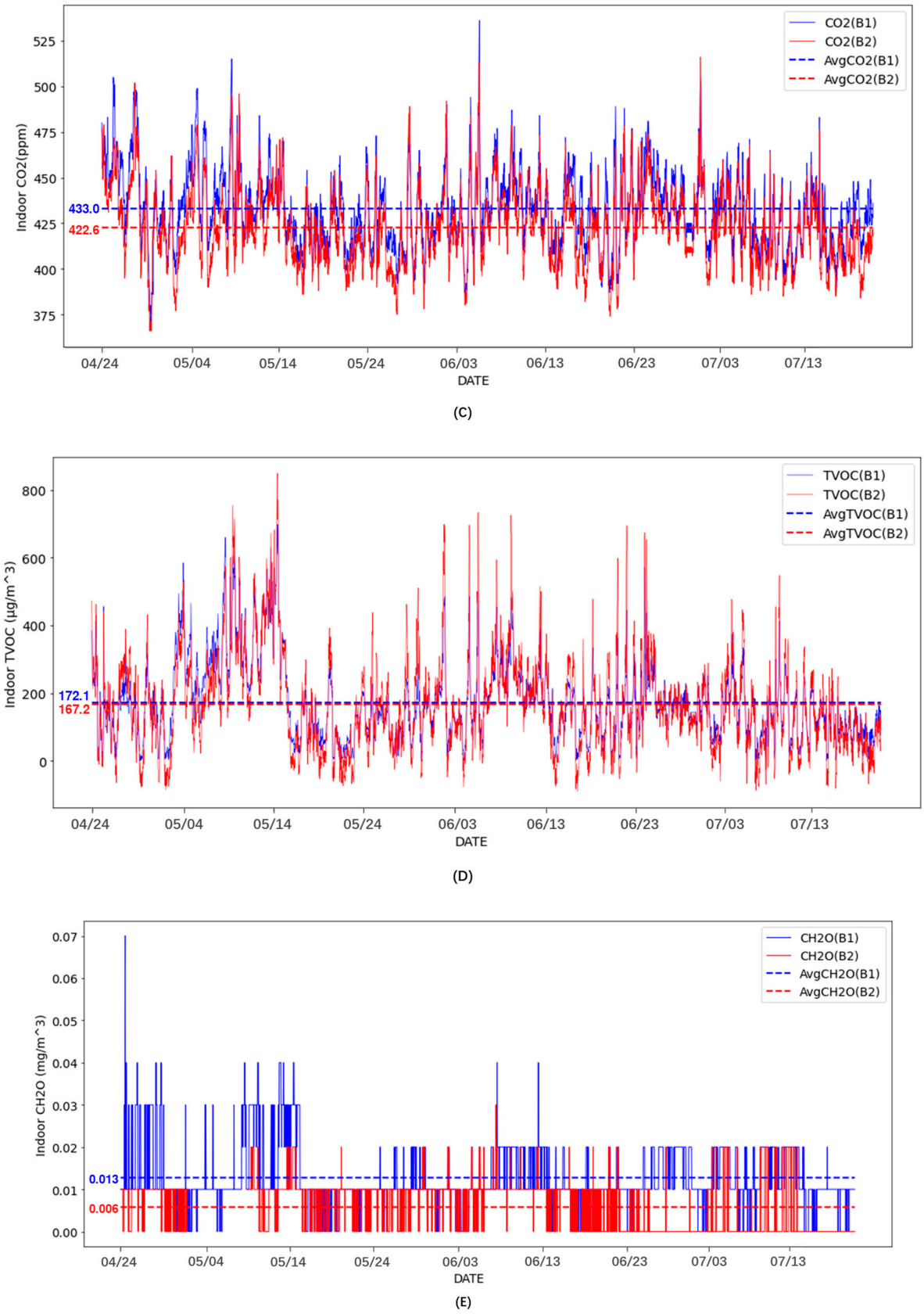

Figure 9. Comparison of indoor and outdoor air pollutant concentrations. (**A**) $PM_{2.5}$, (**B**) PM_{10}, (**C**) CO_2, (**D**) TVOC, (**E**) CH_2O.

3.2.1. Particulate Matter

$PM_{2.5}$ refers to particulate matter with a diameter measuring less than 2.5 microns, originating from combustion of fossil fuels, vehicle exhausts, decoration dust, and kitchen smoke. PM_{10} refers to particulate matter with a diameter measuring no greater than 10 microns, originating from road dust, construction dust, and coal dust. Studies have shown that greening induces an adsorption effect for $PM_{2.5}$ and PM_{10} [23]. Due to window ventilation, more sizeable particulate matter contributes to a greater horizontal force, resulting in its more rapid movement compared to smaller particulate matter. In this study, the implication was that the more sizeable particulate matter rapidly moved outdoors, while particulate matter with a smaller diameter remained indoors. Thus, in general, indoor $PM_{2.5}$ concentrations were higher than outdoor ones, while indoor PM_{10} concentrations were lower.

Our experimental results showed that the range of oscillation in $PM_{2.5}$ in B2 was 3.0~94.5 $\mu g/m^3$ (average: 33.3 $\mu g/m^3$), while that of PM_{10} in B2 was 3.0~100.0 $\mu g/m^3$ (average: 38.8 $\mu g/m^3$). However, the range of $PM_{2.5}$ in B1 was 4.5~103.5 $\mu g/m^3$ (average: 39.9 $\mu g/m^3$), while that of PM_{10} in B1 was 4.5~111.5 $\mu g/m^3$ (average: 46.1 $\mu g/m^3$) (Figure 9A,B). As the whole, the variations in indoor $PM_{2.5}$ and PM_{10} concentrations corresponded consistently with the outdoor variations. The average concentration of indoor $PM_{2.5}$ in B1 and B2 was higher than that of outdoor $PM_{2.5}$ (respectively, 7.3 $\mu g/m^3$ and 0.7 $\mu g/m^3$). In contrast, the average concentration of indoor PM_{10} was lower than that of outdoor PM_{10} (respectively, 6.4 $\mu g/m^3$ and 13.7 $\mu g/m^3$). Further comparative analysis of B2 (with an indoor VGS) and B1 (without an indoor VGS) demonstrated the role of the VGS in lowering the average $PM_{2.5}$ concentration by 16.5% and the average PM_{10} concentration by 15.8%.

3.2.2. Carbon Dioxide

CO_2 is produced from the combustion of coals, oil, natural gases, and other chemical fuels. In addition, humans, animals, and plants exhale CO_2 as part of their metabolism. CO_2 can be absorbed by green plants in exchange for O_2 through photosynthesis, maintaining the atmospheric carbon–oxygen balance.

Our experimental results showed that the CO_2 concentration in B2 ranged from 366.0 to 516.0 ppm (average: 422.6 ppm), while that in B1 ranged from 369.0 to 536.0 ppm (average: 433.0 ppm) (Figure 9C). Comparative analysis of B2 (with an indoor VGS) and B1 (without an indoor VGS) demonstrated the role of the VGS in lowering the average CO_2 concentration by 2.4%, highlighting its utility in improving the IAQ.

3.2.3. Organic Pollutants

Indoor air pollutants primarily comprise CH_2O, NH_3, Rn, C_6H_6, and TVOC and originate from various decoration materials and furniture. Studies have shown that greening can be applied in air purification [17]. Specifically, our research focused on the monitoring of the indoor CH_2O and TVOC concentrations in B1 and B2. Our experimental results showed that the TVOC concentrations in both rooms were similar: the average values of 172.1 and 167.2 $\mu g/m^3$ differed by 2.8% (Figure 9D).

However, the CH_2O concentrations differed markedly between the rooms. The variations in B1 ranged from 0 to 0.07 mg/m^3 (average: 0.013 mg/m^3), while those in B2 ranged from 0 to 0.03 mg/m^3 (average: 0.006 mg/m^3) (Figure 9E). Comparative analysis of B2 (with an indoor VGS) and B1 (without an indoor VGS) demonstrated the role of the indoor VGS in lowering not only the average CH_2O concentration by 53.8% but also the range of oscillations in the CH_2O concentration by 57.1%.

4. Discussion

Based on the various indicator monitoring data, this section discusses the effects of greening systems on indoor thermal comfort, indoor thermal inertia, IAQ, and building energy consumption in relation to different variables (types of rooms, types of indicators, and time). Here, the analysis of the thermal environment revolves around only the data for group A during the transitional season (from 24 April to 25 May), while the analysis of the indoor pollutants revolves around only the data for group B during the transition season and summer (from 24 April to 22 July). The corresponding evaluative parameters for indoor variables were as follows: indoor thermal comfort (predicted mean vote (PMV) and predicted percentage of dissatisfaction (PPD)); indoor thermal inertia (fluctuations in indoor air temperatures and delay times); IAQ (fluctuation ranges and medians of the concentrations of five air pollutants); and building energy consumption (monthly electricity consumption and measurements of its three sub-items; i.e., air conditioning, lighting and sockets, and special electricity). Lastly, this discussion also draws analytical inferences from the comparison of the indicators, their correlations, and the causes underlying the observations.

4.1. Impacts of VGSs on Indoor Thermal Comfort

The analysis of indoor thermal comfort involved rooms A1 (without an external VGS) and A2 (with an external VGS) from group A during the transition season (from 24 April to 25 May). In the calculations in this research, the metabolic rate of a sedentary person in the meeting room was set as 1.2 met (70.0 W/m^2). The thermal insulation of clothing was set at 0.75 clo. for the transition season, as suggested by the ASHRAE Standard 55–2017 [39]. Additionally, practical test results revealed that the measured air velocities were 0.2 m/s in both rooms during the transition season.

The ranges of the oscillations in the PMV and PPD values for A2 were evidently smaller than those for A1 (Figure 10). According to ISO 7730 [36], a given indoor thermal environmental design can be defined with three categories (A–C), each of which prescribes the range of PMV and the maximum PPD that should be achieved in the indoor thermal environment. For category C, the indoor PMV should range from −0.7 to +0.7 and the PPD should be lower than 15.0%.

Our results showed that, over the period spanning 768 h, A2 met the category C criterion for 726 h (average PPD: 10.0%); however, A1 only met the criterion for 681 h (average PPD: 12.0%). Such observations suggested that the external VGS could prolong the period of indoor thermal comfort by 6.6% and mitigate thermal dissatisfaction by 2.0% during the transition season in the absence of air conditioning. Furthermore, during the daytime (from 7:00 a.m. to 7:00 p.m.), A2 met the category C criterion for 388 h and A1 for 347 h, suggesting that the external VGS could enhance daytime thermal comfort by 11.8%. Collectively, these findings emphasised the crucial role of the external VGS in improving indoor thermal comfort in the transition season, especially during the daytime. With the employment of air conditioning systems for indoor thermal comfort, an external VGS could also reduce their operation time by 6.6% for a building occupied for the whole day and 11.8% for a daytime-occupied building, translating into energy savings [40].

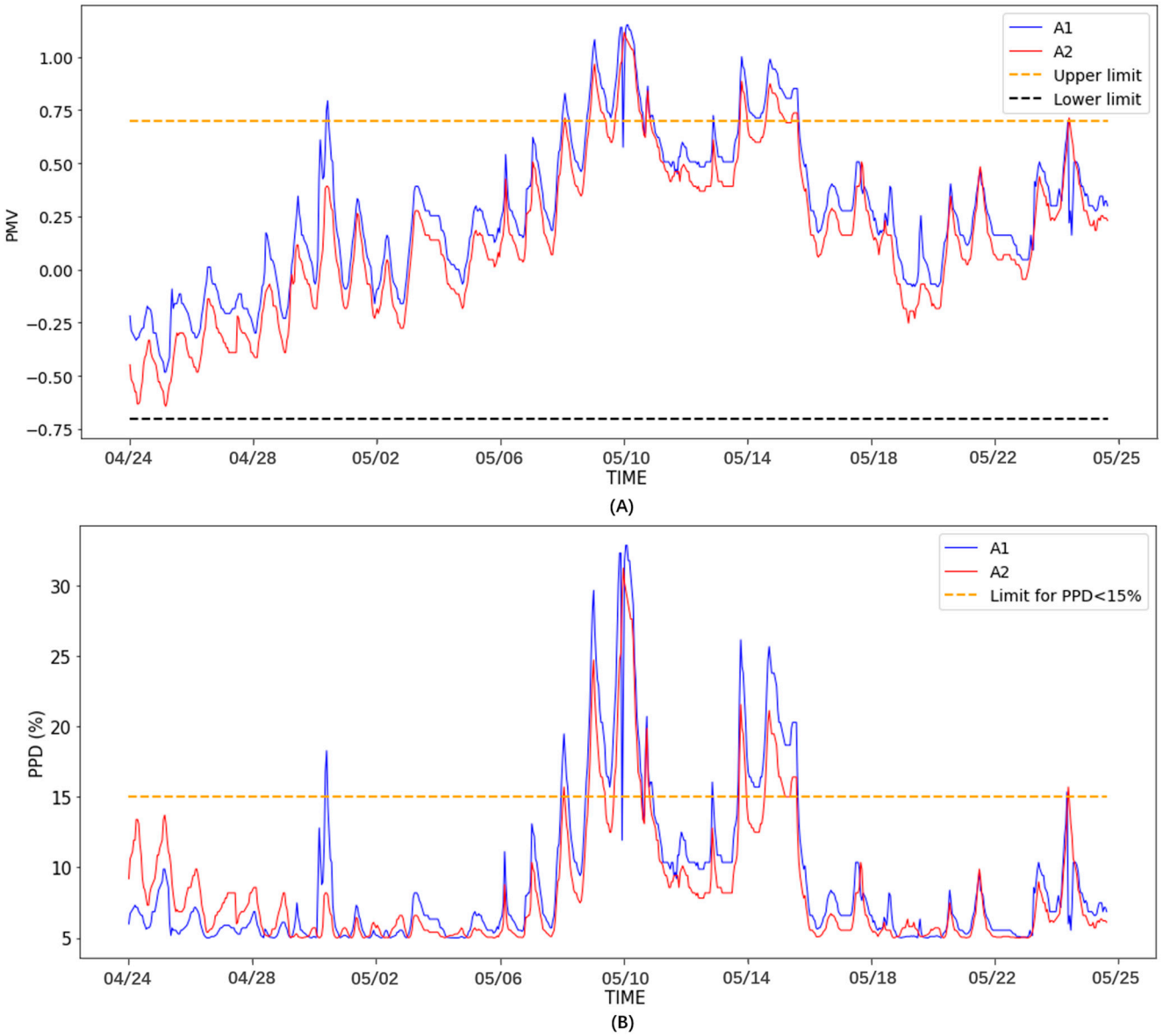

Figure 10. Comparison of indoor thermal comfort evaluation indexes. (**A**) PMV, (**B**) PPD.

4.2. Impacts of VGSs on Thermal Inertia

In order to minimize the potential impact of the interaction between the building greening system and the ground [41,42], a comparison of the rooms in group B on the first floor is not included in this section. Analysis of the thermal inertia involved a comparison of the thermal indicators for A1 (without a VGS) and A2 (with VGS) in group A on the second floor. Specifically, the aim of this study was to investigate the impact of VGSs on thermal inertia. The VGSs were used to examine changes in thermal performances in the transitional season when air conditioning was not in use from 24 April to 25 May. The air temperatures of A1 were higher than those of A2, with the average air temperature of A1 being 0.5 °C higher than that of A2 (Figure 11).

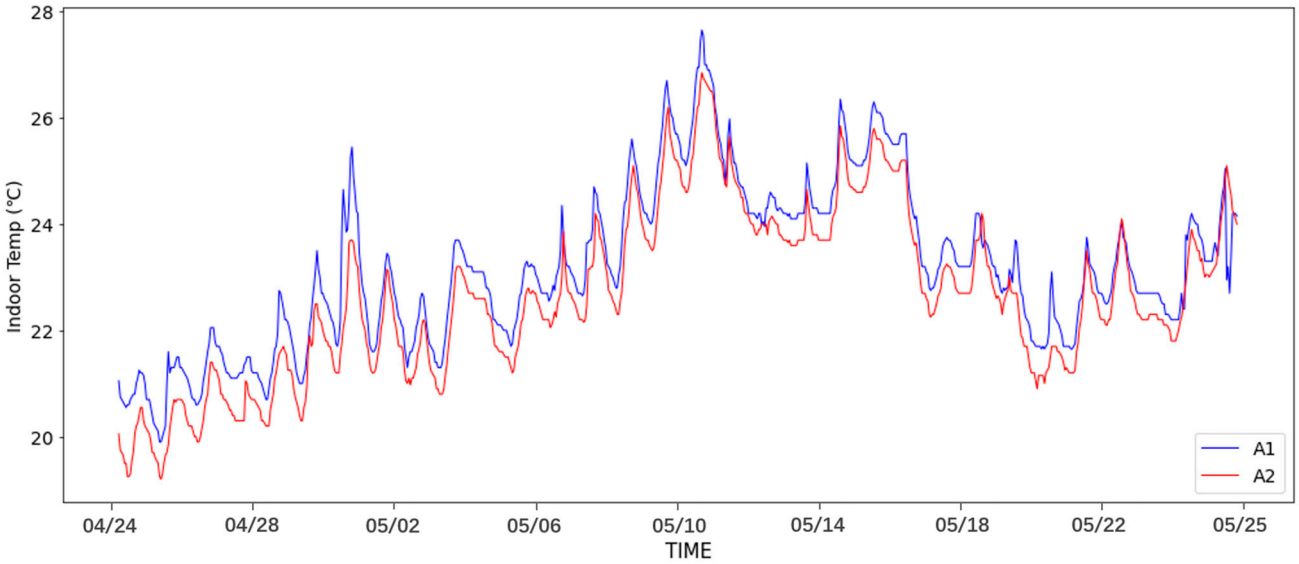

Figure 11. Indoor air temperature curves for the two comparison groups in the transition season.

To examine daily variations in air temperatures and to illustrate the attenuation and delay effects of the building envelopes, two typical days in spring were selected: 27 April, a cloudy day with 0 sunshine hours; and 9 May, a sunny day with 12 sunshine hours. The air temperatures in A1 and A2 exhibited similar variation trends, alongside evident attenuation and delay effects compared to outdoor air temperatures (Figure 12).

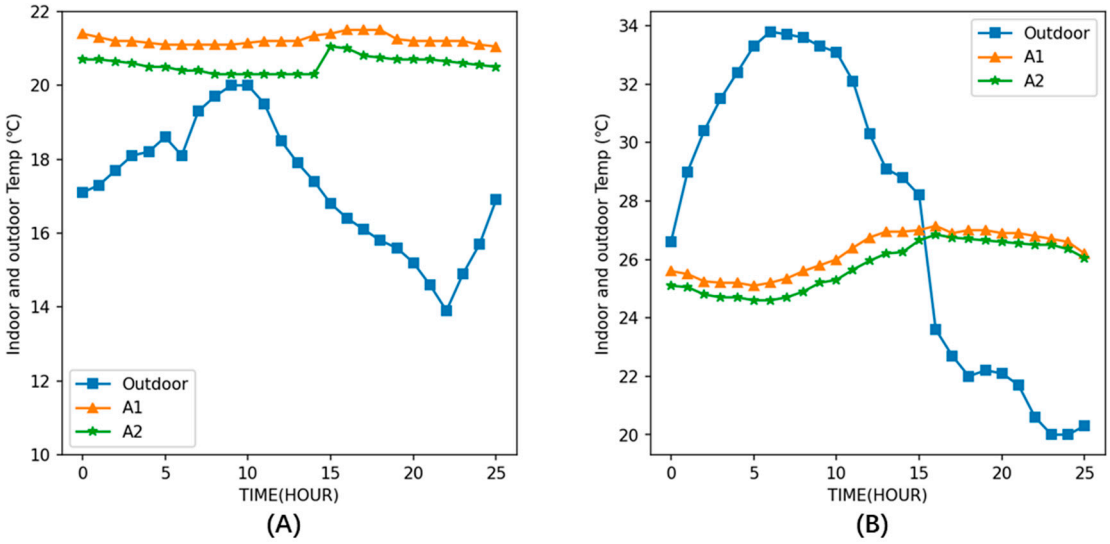

Figure 12. The curves for indoor air temperature on typical days. (**A**) 27th April, (**B**) 9th May.

While the average outdoor air temperature on 27 April was 17.3 °C, the air temperatures of A1 and A2 were higher (respectively, 21.2 °C and 20.6 °C). In contrast, while the average outdoor air temperature on 9 May was 27.5 °C, the air temperatures of A1 and A2 were lower (26.2 °C and 25.8 °C). More specifically, A2 outperformed A1 in terms of thermal protection and heat insulation from the outdoor environment because of the presence of the VGS. These differential findings highlighted the thermal insulation provided by the building envelopes and the VGS, using which indoor air temperatures could be decreased by nearly 1.0 °C.

To analyse the effects of the VGS on the thermal inertia index, the delay time and the thermal attenuation coefficient for group A from 24 April to 25 May were calculated.

The delay time for A2 was found to be larger than that for A1 (Figure 13). Moreover, the average values for the delay time (φ_max/H and φ_min/H) and attenuation coefficient (f) for group A (Table 4) offer corroborating evidence for the above conclusions. The average thermal attenuation coefficient for A2 was 19.5% larger than that for A1. Additionally, the average delay time for A2 was 41.0% greater than that for A1. In summary, A2, which had the greening façade, registered greater thermal inertia, underlining that the VGS could effectively improve the thermal inertia of the building envelope.

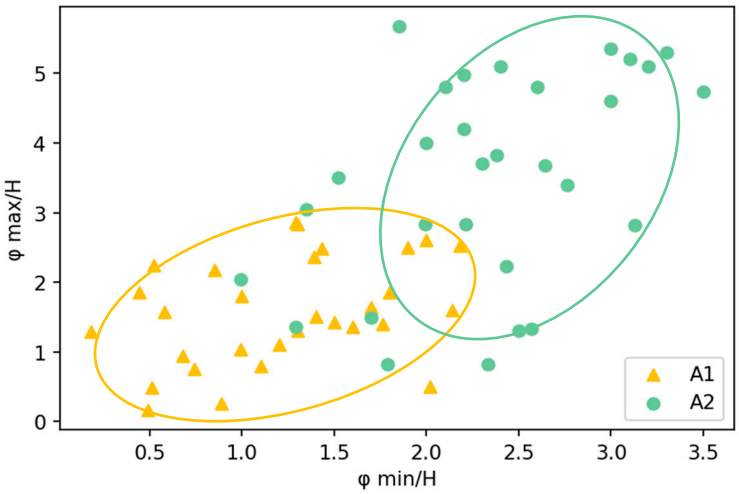

Figure 13. Scatter clustering plot of delay time.

Table 4. Average values for the thermal inertia indexes for comparison group A.

Group ID	Point ID	Average f	Average φ_max/H	Average φ_min/H
Group A	A1	0.87	1.66	1.56
	A2	0.70	2.95	2.20

4.3. Impacts of VGSs on Indoor Air Quality

The analysis of the IAQ involved a comparison of the data-monitoring results for five indicators ($PM_{2.5}$, PM_{10}, CH_2O, TVOC, and CO_2) for B1 (with an external VGS but no indoor VGS) and B2 (with an indoor VGS and potted plants) in group B (Table 5). Firstly, inspection of the box plots (Figure 14) revealed that, for both $PM_{2.5}$ and PM_{10}, the maximum, minimum, and median values for room B2 were lower than those for room B1 (Figure 14A,B), suggesting that the indoor VGS and potted plants substantially promoted adsorption of and reductions in indoor particulate matter. The median indoor $PM_{2.5}$ was higher than that for outdoors, whereas the median indoor PM_{10} was lower, which was attributed to the different sources of indoor $PM_{2.5}$ and PM_{10}. Secondly, for TVOC, the median monitoring value for B1 was 150.5 and that for B2 was 148.0 (Figure 14C); the difference was thus insignificant. However, for CH_2O, the ranges of the oscillations in B1 and B2 evidently differed: compared with the CH_2O in B1, the maximum CH_2O in B2 decreased by 61.5% and the median decreased by 33.3% (Figure 14D). These observations demonstrated that indoor greening critically reduced CH_2O but not TVOC. The reason was that CH_2O represents a single pollutant, whereas TVOC represents an aggregate of different pollutants. In this context, the role of greening in lowering TVOC warrants further investigation. Lastly, the median CO_2 value of 421.0 ppm in B2 differed by about 2.4% from the median CO_2 value of 431.5 ppm in B1 (Figure 14E). This demonstrated the positive effect of indoor greening in reducing indoor CO_2 by photosynthesis. If indoor greening could be further scaled up, CO_2 would be reduced more substantially.

Table 5. Indoor and outdoor air pollutant monitoring data analysis for comparison group B.

Index	Point ID	Minima	Median	Maxima
$PM_{2.5}$ ($\mu g/m^3$)	B1	4.50	39.00	103.50
	B2	3.00	32.50	94.50
	Outdoor	4.00	28.00	108.00
PM_{10} ($\mu g/m^3$)	B1	4.50	46.00	111.50
	B2	3.00	36.50	100.00
	Outdoor	8.00	46.00	211.00
CO_2 (ppm)	B1	369.00	431.50	536.00
	B2	366.00	421.00	516.00
TVOC ($\mu g/m^3$)	B1	5.00	150.50	900.00
	B2	3.00	148.00	846.00
CH_2O (mg/m^3)	B1	0.00	0.02	0.07
	B2	0.00	0.01	0.03

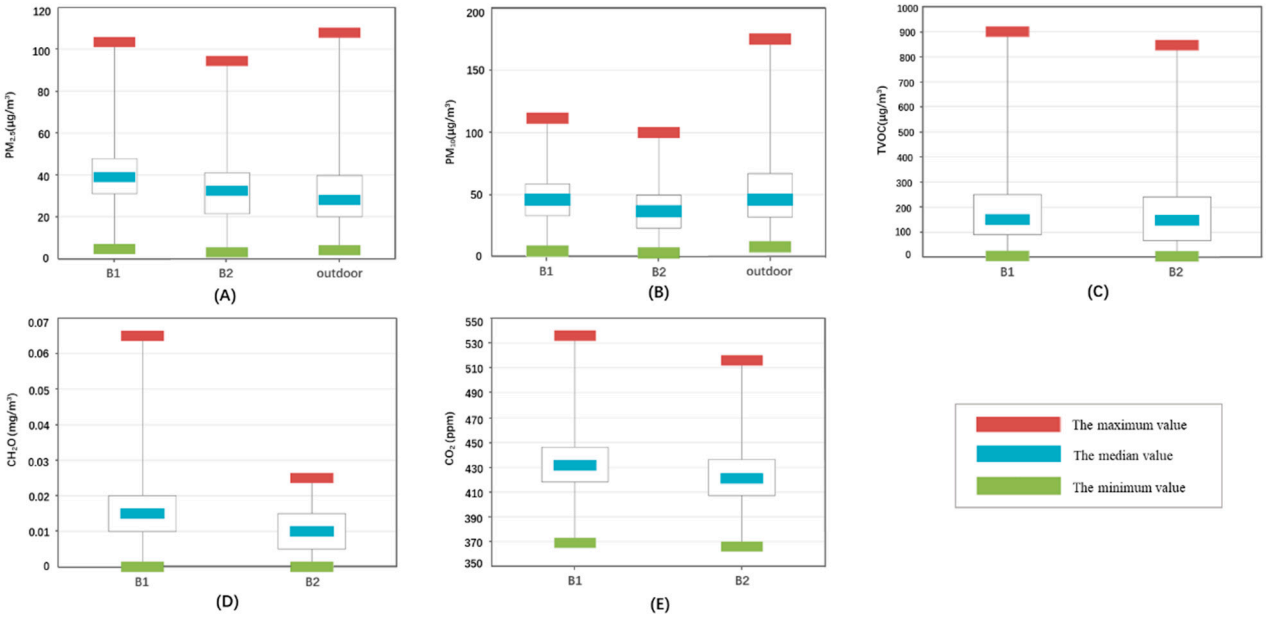

Figure 14. Box plots for indoor air pollutant concentrations. (**A**) $PM_{2.5}$, (**B**) PM_{10}, (**C**) TVOC, (**D**) CH_2O, (**E**) CO_2.

The critical roles of indoor greening in absorbing and reducing the five air pollutants were demonstrated by the fact that, under the same experimental conditions, the values for all five indicators for B2 were lower than those for B1. The most evident improvement was noted for CH_2O, underlining that indoor greening represents a simple but effective way to reduce CH_2O concentrations generated by indoor decorations [43]. Moreover, indoor greening was found to more effectively lower the concentrations of larger particulate pollutants than those of smaller ones: this was reflected by the decline in the median $PM_{2.5}$ and PM_{10} values for B2 by 16.7% and 20.7%, respectively, as compared to B1. Given the predominantly outdoor origins of PM_{10} [22], there is a higher risk of an influx of PM_{10} when the windows of buildings are opened for ventilation. In this context, indoor greening could ensure that the concentrations of indoor large-particulate pollutants remain at acceptable levels.

4.4. Energy Consumption

To analyse the energy savings in this research, actual energy-consumption data for one year of the operation of the building were collected. The annual electricity consumption of the site in this research in 2021 was 141,094 kWh, and the electricity consumption per

unit area was 32.5 kWh/(m^2·a). Since the exhibition zone was not fully operational, the office zone (occupying about 55.0% of the building area) accounted for approximately 80.0% of the electricity consumption. The electricity consumption per unit area of the office zone was calculated as 46.5 kWh/(m^2·a). In accordance with the Standard for Energy Consumption of Buildings GB/T 51161-2016 from the National Standards of the People's Republic of China, the energy-consumption index in this project was lower than both the constraint value (70.0 kWh/(m^2·a)) and the guide value (55.0 kWh/(m^2·a)) for public buildings in a hot summer and cold winter climate zone. Compared with the average energy consumption of similar buildings (around 65.0 kWh/(m^2·a)), the results from our research could translate into energy savings of at least 25.0%.

In terms of the monthly power consumption and the sub-item analysis (Figure 15), the power consumption in summer was evidently lower than that in winter. Furthermore, the power consumption for air conditioners in the transition season was the lowest over the year, especially in May, for which the power consumption was only 593.0 kWh.

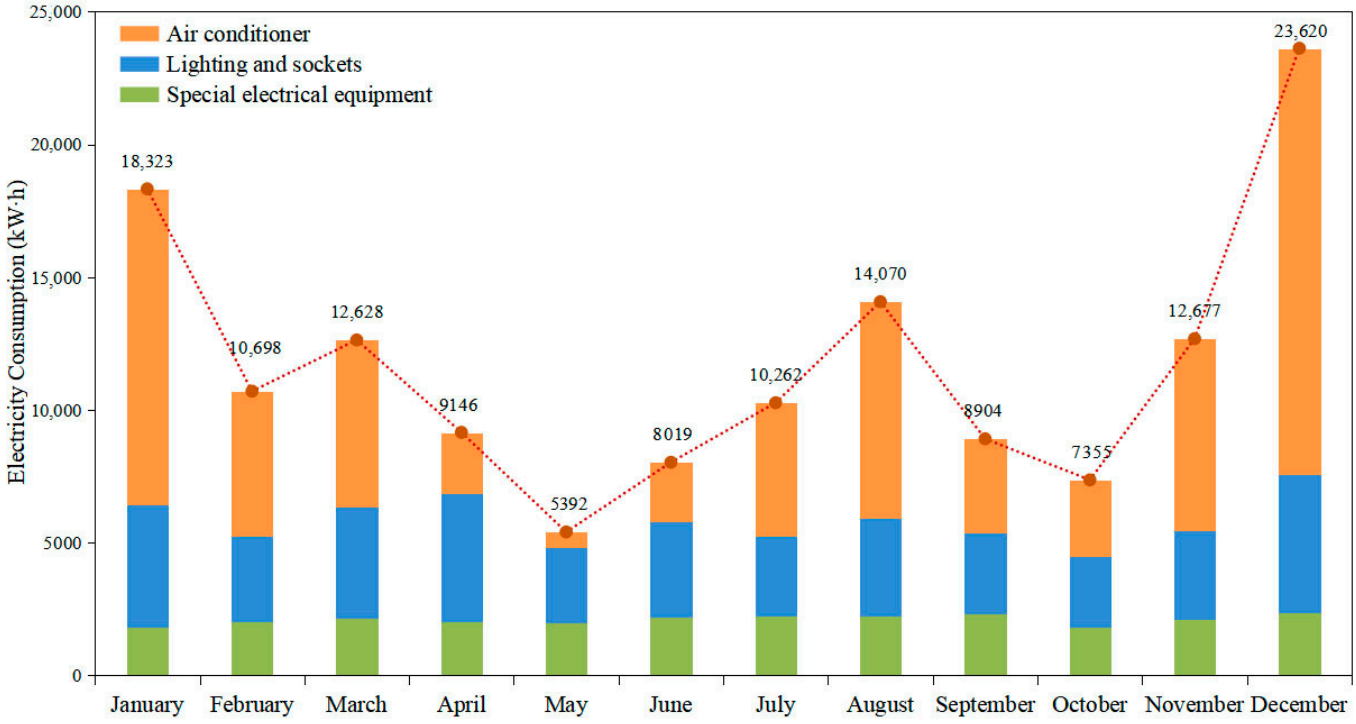

Figure 15. Monthly electricity consumption and sub-item analysis.

As the building was in use throughout the experimental period, numerous other factors might have affected its energy consumption. Therefore, in contrast to experimental buildings, the effects of greening systems on energy conservation in this operational building could not be accurately quantified. Nonetheless, the data overwhelmingly suggested that the reduced energy consumption for air conditioning during the transition season and summer contributed critically to the overall energy conservation achieved in the project. Such findings collectively highlight the importance of the heat insulation and cooling effects provided by greening systems for energy conservation.

5. Conclusions

In this study, the impacts of external and indoor vertical greening systems (VGSs) on building green performances were investigated with a focus on the thermal environment, indoor air quality, and energy consumption. Through real-time monitoring and data analysis of a green-certified building in Changzhou, China, numerous insightful conclusions could be drawn as follows:

(1) Through the use of the external VGS, optimisation of the indoor thermal environment was observed in the comparison groups. In the presence of the VGS, the average indoor air temperatures decreased by up to 0.7 °C in the transition season and by up to 0.6 °C in summer. Calculations further revealed that the external VGS could prolong the period of indoor thermal comfort by 6.6%, mitigate thermal dissatisfaction by 2.0% in the transition season, and shorten the operation time of air conditioning by up to 11.8%. Additionally, the room with a greening facade registered a greater thermal inertia, and the increases in both the thermal attenuation coefficient (by 19.5%) and the delay time (by 41.0%) demonstrated that the VGS could effectively improve the thermal inertia of the building envelope;
(2) Analysis of the effects of the indoor VGS on the IAQ indicators revealed that lower air-pollutant concentrations were obtained in the presence of the VGS. Improvements were most pronounced for PM and CH_2O. In the presence of the indoor VGS, the median $PM_{2.5}$ and PM_{10} concentrations declined by 16.7% and 20.7%, respectively, while the median CH_2O concentrations declined by 33.3%. Such findings attest to the positive effects of indoor greening in absorbing and reducing air pollutants;
(3) Statistical analysis of the annual power consumption of the project revealed energy savings of up to 25% for the building with the VGSs compared to similar buildings without any VGSs. Moreover, the VGSs enabled a reduction in energy consumption for air conditioning during the transition season and summer, underlining its role in energy conservation.

Our research demonstrated that greening systems applied to building envelopes and indoor spaces offer quantifiable benefits in terms of numerous parameters, including thermal properties, indoor air quality, and energy conservation. It is thus envisioned that VGSs could be integrated as a green strategy into architectural designs and urban planning in order to optimise building green performances and regulate urban microclimates.

It is worth noting that this research was based on an actual operational building under the influences of complex factors, and the experimental measurements might not have been as rigorous as laboratory-based ones. However, the conclusions have both practical and referential utility, especially regarding the effects of VGSs on actual operational buildings.

In our future work, the experimental design will be continuously optimized to minimize the interference of building operations on the experimental data. In addition, the experiment will be implemented over a longer time period to cover all seasons, and investigations of the interaction between the building VGSs and the surrounding environment, including the ground and landscape greening system, will continue in order to study the contributions of VGSs in a more comprehensive manner.

Author Contributions: Y.Y. and Y.L. were responsible for the overall conceptual design and the development of the research methods. K.H., Z.W. and K.D. were responsible for the implementation of the experiment, data analysis, and the writing of the manuscript. P.L. and X.S. was responsible for the project administration. All authors have read and agreed to the published version of the manuscript.

Funding: This research was funded by the Carbon Emission Peak and Carbon Neutrality Innovative Science Foundation of Jiangsu Province: "The key research and demonstration projects of future low-carbon emission buildings" (no. BE2022606).

Institutional Review Board Statement: Not applicable.

Informed Consent Statement: Not applicable.

Data Availability Statement: Data available on request due to privacy. The data presented in this study are available on request from the corresponding author. The data are not publicly available due to the data is classified.

Acknowledgments: The authors are grateful for the support relating to translation and project investigation provided by colleagues and friends.

Conflicts of Interest: The authors declare that the research was conducted in the absence of any commercial or financial relationships that could be construed as potential conflicts of interest.

Nomenclature

Abbreviations

IEQ	indoor environmental quality
VGS	vertical greening system
GW	green wall
GF	green facade
LWS	living wall system
IAQ	indoor air quality
IoT	Internet of Things
RH	relative humidity
TVOC	total volatile organic compounds
CH_2O	formaldehyde
PMV	predicted mean vote
PPD	predicted percentage of dissatisfaction
EPS	expanded polystyrene
VRV	variable refrigerant volume
IPLV	integrated part load value
$PM_{2.5}$	particulate matter 2.5
PM_{10}	particulate matter 10
CO_2	carbon dioxide
MQTT	message queuing telemetry transport

Parameters

φ_{max}	the maximum delay time, H
φ_{min}	the minimum delay time, H
$\varphi_{max,in}$	the time with the maximum indoor air temperature, H
$\varphi_{max,out}$	the time with the maximum outdoor air temperature, H
$\varphi_{min,in}$	the time with the minimum indoor air temperature, H
$\varphi_{min,out}$	the time with the minimum outdoor air temperature
$T_{max,in}$	the maximum indoor air temperature, °C
$T_{min,in}$	the minimum indoor air temperature, °C
$T_{max,out}$	the maximum outdoor air temperature, °C
$T_{min,out}$	the minimum outdoor air temperature, °C

References

1. Rowe, T.; Poppe, J.; Buyle, M.; Belmans, B.; Audenaert, A. Is the sustainability potential of vertical greening systems deeply rooted? Establishing uniform outlines for environmental impact assessment of VGS. *Renew. Sustain. Energy Rev.* **2022**, *162*, 112414. [CrossRef]
2. Du, H.; Cai, W.; Xu, Y.; Wang, Z.; Wang, Y.; Cai, Y. Quantifying the cool island effects of urban green spaces using remote sensing Data. *Urban For. Urban Green* **2017**, *27*, 24–31. [CrossRef]
3. Yang, L.; Zhang, L.; Li, Y.; Wu, S. Water-related ecosystem services provided by urban green space: A case study in yixing city (China). *Landsc. Urban Plann.* **2015**, *136*, 40–51. [CrossRef]
4. Pugh, T.; MacKenzie, A.; Whyatt, J.; Hewitt, N.C. Effectiveness of green infrastructure for improvement of air quality in urban street canyons. *Environ. Sci. Technol.* **2012**, *46*, 7692–7699. [CrossRef] [PubMed]
5. Manso, M.; Teot´onio, I.; Silva, C.M.; Cruz, C.O. Green roof and green wall benefits and costs: A review of the quantitative evidence. *Renew. Sustain. Energy Rev.* **2020**, *135*, 110111. [CrossRef]
6. Ascione, F.; De Masi, R.F.; Mastellone, M.; Ruggiero, S.; Vanoli, G.P. Green walls, a critical review: Knowledge gaps, design parameters thermal performances and multicriteria design approaches. *Energies* **2020**, *13*, 2296. [CrossRef]
7. Yang, F.; Yuan, F.; Qian, F.; Zhuang, Z.; Yao, J. Summertime thermal and energy performance of a double-skin green facade: A case study in Shanghai. *Sustain. Cities Soc.* **2018**, *39*, 43–51. [CrossRef]
8. Raji, B.; Tenpierik, M.J.; van den Dobblesteen, A. The impact of greening systems on building energy performance. *Renew. Sustain. Energy Rev.* **2015**, *45*, 610–623. [CrossRef]
9. Coma, J.; Perez, G.; de Gracia, A.; Bures, S.; Urrestarazu, M.; Cabezza, L.F. Vertical greenery systems for energy savings in buildings: A comparative study between green walls and green facades. *Build. Environ.* **2017**, *111*, 228–237. [CrossRef]
10. Thomsit, F.; Essah, E.A.; Hadley, P.; Blanusa, T. The impact of green facades and vegetative cover on the temperature and relative humidity within model buildings. *Build. Environ.* **2020**, *181*, 107009. [CrossRef]
11. Dahanayake, K.W.D.K.C.; Chow, C.L. Studying the potential of energy saving through vertical greenery systems. *Energy Build.* **2017**, *138*, 47–59. [CrossRef]
12. Olivieri, F.; Olivieri, L.; Neila, J. Experimental study of the thermal-energy performance of an insulated vegetal facade under summer conditions in a continental mediterranean climate. *Build. Environ.* **2014**, *77*, 61–76. [CrossRef]
13. Chen, Q.; Li, B.; Liu, X. An experimental evaluation of the living wall system in hot and humid climate. *Energy Build.* **2013**, *61*, 298–307. [CrossRef]

14. Haggag, M.; Hassan, A.; Elmasry, S. Experimental study on reduced heat gain through green façades in a high heat load climate. *Energy Build.* **2014**, *82*, 668–674. [CrossRef]
15. Pichlhfer, A.; Sesto, E.; Hollands, J.; Korjenic, A. Health-Related Benefits of Different Indoor Plant Species in a School Setting. *Sustainability* **2021**, *13*, 9566. [CrossRef]
16. Weerakkody, U.; Dover, J.W.; Mitchell, P.; Reiling, K. Evaluating the impact of individual leaf traits on atmospheric particulate matter accumulation using natural and synthetic leaves. *Urban For. Urban Green.* **2008**, *30*, 98–107. [CrossRef]
17. Przybysz, A.; Sæbø, A.; Hanslin, H.M.; Gawronski, S.W. Accumulation of particulate matter and trace elements on vegetation as affected by pollution level, rainfall and the passage of time. *Sci. Total Environ.* **2010**, *481*, 360–369. [CrossRef]
18. Ottele, M.; van Bohemen, H.D.; Fraaji, A.L.A. Quantifying the deposition of particulate matter on climber vegetation on living walls. *Ecol. Eng.* **2010**, *36*, 154–162. [CrossRef]
19. Ysebaert, T.; Koch, K.; Samson, R.; Denys, S. Green walls for urban particulate matter pollution—A review. *Urban For. Urban Green.* **2021**, *59*, 127014. (In Chinese) [CrossRef]
20. Feng, H.; Hewage, K. Lifecycle assessment of living walls: Air purification and energy performance. *J. Clean. Prod.* **2014**, *69*, 91–99. [CrossRef]
21. Yang, J.; Yu, Q.; Gong, P. Quantifying air pollution removal by green roofs in Chicago. *Atmos. Environ.* **2008**, *42*, 7266–7273. [CrossRef]
22. Sternberg, T.; Viles, H. Dust particulate absorption by ivy (*Hedera helix* L.) on historic walls in urban environments. *Sci. Total Environ.* **2010**, *409*, 162–168. [CrossRef]
23. He, C.; Qiu, K.; Alahmad, A.; Pott, R. Particulate matter capturing capacity of roadside evergreen vegetation during the winter season. *Urban For. Urban Green* **2020**, *48*, 126510. [CrossRef]
24. Alexandri, E.; Jones, P. Temperature decreases in an urban canyon due to green walls and green roofs in diverse climates. *Build Environ.* **2008**, *43*, 480–493. [CrossRef]
25. Mazzali, U.; Peron, F.; Romagnoni, P.; Pulselli, R.M.; Bastianoni, S. Experimental investigation on the energy performance of Living Walls in a temperate climate. *Build Environ.* **2013**, *64*, 57–66. [CrossRef]
26. Sailor, D. A green roof model for building energy simulation programs. *Energy Build.* **2008**, *40*, 1466–1478. [CrossRef]
27. Altan, H.; John, N.; Yoshimi, J. Comparative Life Cycle Analysis of Green Wall Systems in the UK. In Proceedings of the 2nd International Sustainable Buildings Symposium, Ankara, Turkey, 28–30 May 2015; p. 10.
28. Magrassi, F.; Perini, K. Environmental and Energetic Assessment of a Vertical Greening System Installed in Genoa. In Proceedings of the International Conference Urban Comfort and Environmental Quality, Genoa, Italy, 28–29 September 2017; pp. 132–136.
29. Ottele, M.; Perini, K.; Haas, E.M. 19—Life cycle assessment (LCA) of green façades and living wall systems. In *Eco-Efficient Construction and Building Materials*; Pacheco-Torgal, F., Cabeza, L.F., Labrincha, J., de Magalhaes, A., Eds.; Woodhead Publishing: Sawston, UK, 2014; pp. 457–483.
30. Natarajan, M.; Rahimi, M.; Sen, S.; Mackenzie, N.; Imanbayev, Y. Living wall systems: Evaluating life-cycle energy, water and carbon impacts. *Urban Ecosyst.* **2015**, *18*, 1–11. [CrossRef]
31. Pan, L.; Chu, L.M. Energy saving potential and life cycle environmental impacts of a vertical greenery system in Hong Kong: A case study. *Build Environ.* **2016**, *96*, 293–300. [CrossRef]
32. Chafer, M.; Perez, G.; Coma, J.; Cabeza, L.F. A comparative life cycle assessment between green walls and green facades in the Mediterranean continental climate. *Energy Build.* **2021**, *249*, 111236. [CrossRef]
33. Zhang, G.; He, B. Towards green roof implementation: Drivers, motivations, barriers and recommendations. *Urban For. Urban Green.* **2021**, *58*, 126992. [CrossRef]
34. Cao, Y.; Xu, C.; Kamaruzzaman, S.N.; Aziz, N.M. A Systematic Review of Green Building Development in China: Advantages, Challenges and Future Directions. *Sustainability* **2022**, *14*, 12293. [CrossRef]
35. Anand, P.; Sekhar, C.; Cheong, D.; Santamouris, M. Occupancy-based zone-level VAV system control implications on thermal comfort, ventilation, indoor air quality and building energy efficiency. *Energy Build.* **2019**, *204*, 109473. [CrossRef]
36. *ISO 7730:2005*; Ergonomics of the Thermal Environment—Analytical Determination and Interpretation of Thermal Comfort Using Calculation of the PMV and PPD Indices and Local Thermal Comfort Criteria. ISO: Geneva, Switzerland, 2005.
37. Baglivo, C.; Congedo, P.; Fazio, A.; Laforgia, D. Multi-objective optimization analysis for high efficiency external walls of zero energy buildings (ZEB) in the Mediterranean climate. *Energy Build.* **2014**, *84*, 483–492. [CrossRef]
38. *QX/T 152-2012*; China Meteorological Administration. Division of Climatic Season. Meteorological Press: Beijing, China, 2012.
39. *ASHRAE Standard 55:2017*; Thermal Environmental Conditions for Human Occupancy. ASHRAE: Atlanta, GA, USA, 2017.
40. Hao, X.; Liu, L.; Tan, H.; Lin, Y.; Hu, J.; Yin, W. The Impacts of Greenery Systems on Indoor Thermal Environments in Transition Seasons: An Experimental Investigation. *Buildings* **2022**, *12*, 506. [CrossRef]
41. Nawalany, G.; Sokolowski, P. Numerical Analysis of the Effect of Ground Dampness on Heat Transfer between Greenhouse and Ground. *Sustainability* **2021**, *13*, 3084. [CrossRef]

42. Sokolowski, P.; Nawalany, G. Experimental study of the impact of the vegetable cold store floor location on heat exchange with the soil. *Appl. Ecol. Environ. Res.* **2019**, *17*, 8179–8189. [CrossRef]
43. Du, L.; Leivo, V.; Prasauskas, T.; Taubel, M.; Martuzevicius, D.; Haverinen-Shaughnessy, U. Effects of Energy Retrofits on Indoor Air Quality in Multifamily Buildings. *Indoor Air* **2019**, *29*, 686–697. [CrossRef]